The Dynamics of a Rock Drill

by

Adriana Davidova
B.Sc., UVic, 1998

A Thesis Submitted in Partial Fulfillment
of the Requirements for the Degree of

Master's of Science

in the Department of Mathematics and Statistics.
We accept this thesis as conforming
to the required standard.

[redacted]

Dr. C. Bose, Department of Mathematics & Statistics, University of Victoria

[redacted]

Dr. R. Edwards, Department of Mathematics & Statistics, University of Victoria

[redacted]

Dr. F. Milinazzo, Department of Mathematics & Statistics, University of Victoria

[redacted]

[redacted] *Dr. J. Haddow, Department of Mechanical Engineering, University of Victoria*

Supervisor: Dr. C.J. Bose

Abstract

This thesis focuses on a model for the movement of a rotary drill, such as that used in oil drilling rigs. Such a rotary drill is typically composed of three intermeshed gears. During operation the drill hits and bounces off the rock, chipping the surface at contact. In order to design more efficient and durable drills, one may ask, for different parts of the wheel, what the long term distribution of hits is, should a stable one exist. To answer this question, A. Lasota and K. Rusek analyzed the movement of one of the wheels, which simplifies the model to two dimensions. Using the Birkhoff ergodic theorem they were able to find an estimate for the long term distribution of hits by computing long orbit averages. However, due to the nature of this method, computer round off error is compounded throughout the numerical process, contributing greatly to the uncertainty of the estimate. This motivates the need for an alternative way of computing the density function for the distribution of hits. The main results of this thesis are a confirmation of the Lasota and Rusek's work, and an alternative and more efficient way of obtaining refined density distribution estimates.

We will begin by discussing the Birkhoff ergodic method, and Lasota and Rusek's model and results. Then, a Markov approximation scheme, known as Ulam's method of computing the density function will be presented. The similar estimate for the density function produced using Ulam's method will support Lasota and Rusek's results. More refined estimates will be computed using the latter method, providing numerical evidence of its stability. Furthermore, we will derive a formula for the drilling efficiency in terms of the rotational speed of the drill. Numerically we will determine the rotational speed that yields maximum drilling efficiency, and observe the asymptotic behaviour of the efficiency for large speeds.

Examiners [redacted]

Dr. C.J. Bose, Department of Mathematics & Statistics, University of Victoria

[redacted]

Dr. R. Edwards, Department of Mathematics & Statistics, University of Victoria

[redacted]

Dr. F. Milinazzo, Department of Mathematics & Statistics, University of Victoria

[redacted]

Dr. J. Haddow, Department of Mechanical Engineering, University of Victoria

Contents

Acknowledgements

The last few years have been challenging, yet rewarding and enjoyable. The experience of writing this thesis has helped me grow not only academically but also personally. As I enter the next phase of my life I feel confident that I can meet any challenge set before me.

I am especially greatful to have had the opportunity to have worked with Dr. Christopher Bose. His vast knowledge and commitment to this project have made its completion possible. His respect, tolerance and motivational skills have helped me a great deal, and have taught me the power of perseverance.

I greatly appreciate the academic as well as personal guidance and support extended to me by Dr. C. Sean Bohun, whose efforts have helped make this project a success.

I dedicate this thesis to my parents.

Chapter 1

Introduction

In this thesis we will study the dynamics of an oil drill, consisting of three or more toothed wheels. Each wheel rotates about its axis, while the drill bit rotates about its vertical axis. For sufficiently high speeds this rotational movement forces the drill bit to jump off and subsequently land back on the surface. As a result, part of the kinetic energy is converted into work, thus providing the drilling action in crushing the rock. Should it exist, the distribution of the points of recontact is important not only from the point of view of drilling, but also for the uniformity of the wear-and-tear of the drill bit. We will present two ways of computing an estimate for the distribution of hits - the Birkhoff ergodic method and Ulam's method and their respective advantages and disadvantages. Using the estimates for the distribution we will predict the asymptotics of the drill's efficiency as the linear speed increases to infinity, as well as the linear speed which yields highest efficiency.

In Chapter 2 we will present the method used by Lasota and Rusek [8]. We begin this discussion by defining and studying the Perron Frobenius operator, which plays a key role in density estimation. The Birkhoff ergodic theorem will be presented and applied to a dynamical system of a given unit interval map in computing an estimate for its invariant measure. This is done by partitioning the unit interval, and

computing a long orbit produced by the map for a randomly chosen initial point. For each set in the partition the frequency at which it is revisited by the orbit will be determined numerically, thus producing a finite dimensional density vector. This is an approximation of the invariant density function. We will point out the drawbacks of this method, motivating the need for an alternative way of estimating the density function given a unit interval map.

Chapter 3 establishes a two-dimensional model for the rock drill, which provides the transformation describing the movement of the wheel in the plane of its rotation. The resulting unit-interval map is studied, and the Birkhoff ergodic method is applied to obtain the density function of the drill map.

Ulam's method of computing the distribution vector is presented in Chapter 4. We will explain how to discretise the Perron-Frobenius operator and obtain a finite dimensional density vector using the transition probability matrix of the transformation of interest. The method is illustrated on the dyadic map, providing a contrast with the Birkhoff Ergodic method discussed in Chapter 2. In addition the dyadic example will provide evidence of the efficiency and accuracy of Ulam's method.

In Chapter 5 we will find estimates for the invariant density function of the rock drill map obtained in Chapter 3 using Monte-Carlo type simulations of Ulam's method. We will observe the fast convergence of this method by studying the percent error function between estimates numerically. The error function will pick up on discontinuities in the invariant density function, a feature which was not detected with the Birkhoff ergodic method. The distribution vector for several values of the linear speed will be estimated. Once a density function is found, we will explain how one can compute the efficiency of the drill (in terms of the drill parameters and speed). The speed which provides highest efficiency will be obtained and the asymptotic behaviour of the dynamics of the drill will be studied numerically.

In Chapter 6 we will summarize the results from the two methods and some future work will be suggested.

Chapter 2

The Birkhoff Ergodic Theorem

2.1 Introduction

In this chapter we will introduce some of the terminology used in this thesis. Here we will begin the study of probability density functions, that is functions describing the probabilistic behaviour of an orbit produced by a given map. An integral part in this discussion is the Perron-Frobenius operator associated with the map. This operator will be introduced here and will be revisited in Chapter 3 and 4.

The Birkhoff Ergodic Theorem will be presented, providing an intuitive way for computing the probability density function of a given map. This will be illustrated on the triadic and dyadic maps.

2.2 Overview of Ergodic Theory

Let $(X, \mathcal{B}, \mu)$ be a measure space. We will call functions $S : X \to X$ *transformations.* Most transformations in this thesis will not be invertible.

Definition 2.1 *A transformation $S : X \to X$ is called* **measurable** *if $A \in \mathcal{B} \Rightarrow S^{-1}(A) \in \mathcal{B}$, where $S^{-1}(A) \equiv \{x \in X : S(x) \in A\}$.*

Definition 2.2 *A measurable transformation $S : X \to X$ is* **measure preserving**

if $\mu(S^{-1}(A)) = \mu(A)$ *for all* $A \in \mathcal{B}$.

Definition 2.3 *Let* S: $X \to X$ *be a measurable transformation. A Borel measure* ν *will be called an* **invariant measure** *for* S *if* S *is measure preserving for* ν.

It is often difficult to check whether S preserves a given measure since one rarely has an explicit knowledge of all members of $\mathcal{B}$. It is therefore useful to define the following family of subsets.

Definition 2.4 *A family* $\mathcal{P}$ *of subsets of* X *is called a* π**-system** *if for any* A, B *in* $\mathcal{P}$ *their intersection* $A \cap B$ *is also in* $\mathcal{P}$. *We say that a* π*-system* **generates** *a* σ*-algebra* $\mathcal{B}$ *if* $\mathcal{B}$ *is the smallest* $\sigma-$*algebra containing* $\mathcal{P}$.

EXAMPLE 1: Let $X = [0,1)$ and μ be Lebesgue measure. Then $\mathcal{P} = \{(a,b) \mid 0 \leq a < b \leq 1\} \cup \{[0,c) \mid 0 < c < 1\} \cup \emptyset$ is a π-system (it is easy to check that it is closed under intersections).

Since every open subset of $[0,1)$ is a countable union of (disjoint) intervals from $\mathcal{P}$ (see [2]), the σ-algebra generated by $\mathcal{P}$ contains all open subsets. It follows that $\mathcal{P}$ generates the Borel σ-algebra.

To check whether a transformation is measure preserving we just need to consider the elements of a generating π-system.

Theorem 2.5 *Let* $S : X \to X$ *be measurable and let* $\mathcal{P}$ *be a* π*-system that generates* $\mathcal{B}$. *Then* S *is measure preserving if* $\mu(S^{-1}(A)) = \mu(A)$ *for all* $A \in \mathcal{P}$.

Proof. Let measure η be defined by $\eta(A) = \mu(S^{-1}(A))$. Then $\mu(A) = \eta(A)$ for all $A \in \mathcal{P}$. But if two measures on $\mathcal{B}$ agree on every element of a given generating π-system then they define the same measure (see Billingsley [6]). Therefore $\mu = \eta$ on $\mathcal{B}$. □

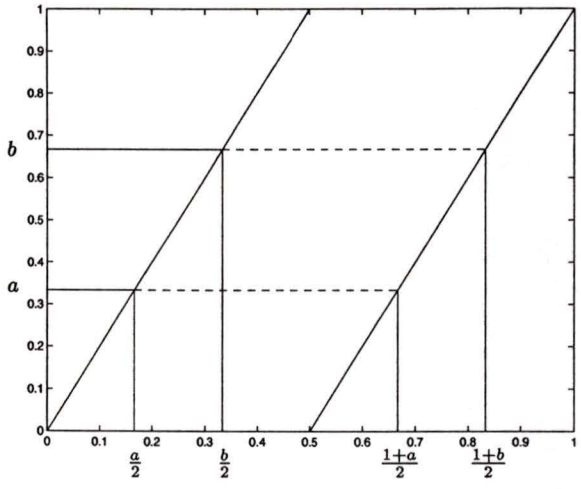

Figure 2.1: The transformation $S(x) = 2x(\text{mod } 1)$ on $[0, 1)$.

We apply this result in the next example.

EXAMPLE 2: Let $X = [0, 1)$, $\mathcal{B}$ = Borel σ-algebra of X and μ = Lebesgue measure. Let $S : X \to X$ be defined by $S(x) = 2x(\text{mod } 1)$, and refer to Figure 2.1. To see that S is measure preserving we show that the measure preserving property holds on the π-system $\mathcal{P} = \{(a, b) \mid 0 \leq a < b \leq 1\} \cup \{[0, c) \mid 0 < c < 1\} \cup \emptyset$. For any element $I \in \mathcal{P}$, $S^{-1}(I)$ consists of two disjoint intervals I_1 and I_2 with $\mu(I_i) = \frac{1}{2}\mu(I)$. Hence $\mu(S^{-1}I) = \mu(I)$.

In order to study the dynamical properties and asymptotics of a given transformation S we need the notion of absolutely continuous invariant measures.

Definition 2.6 *Let $(X, \mathcal{B}, \mu)$ be a measure space. A Borel measure ν on X is* **absolutely continuous** *with respect to the measure μ, denoted $\nu \ll \mu$, if*

$$\nu(A) = 0 \text{ for every } A \in \mathcal{B}(X) \text{ such that } \mu(A) = 0.$$

If $S : X \to X$ is a measurable transformation and ν is invariant under S and is absolutely continuous with respect to μ, then we say that ν is an absolutely

continuous invariant measure, abbreviated acim, with respect to μ. Henceforth, the statement "with respect to the measure μ" will be omitted if it is clear from the context.

Next we look at an example of an absolutely continuous measure with respect to Lebesgue measure.

EXAMPLE 3: Consider the measure space $X = [0, 1]$ equipped with Lebesgue measure μ. Let $f = 2x$ and define the measure ν by

$$\nu(A) = \int_A f d\mu.$$

Then if $\mu(A) = 0$, $\nu(A) = \int_A 2x dx = 0$. Hence $\nu \ll \mu$.

The next theorem shows that this is, essentially, the only way $\nu \ll \mu$ can arise and will provide an invariant density.

Theorem 2.7 *(Radon-Nikodym) Let $(X, \mathcal{B}, \mu)$ be a σ-finite[1] measure space. Let ν be an absolutely continuous measure with respect to μ. Then there exists a nonnegative measurable function f such that for each set $A \in \mathcal{B}(X)$ we have*

$$\nu(A) = \int_A f \, d\mu.$$

The function f is called the **density of** ν *and is unique in the sense that if g is any measurable function with this property then $g = f$, μ-a.e..*

Proof. See [2]. □

REMARK: The function f is also called the **Radon-Nikodym derivative** of ν with respect to μ, and is denoted by $\frac{d\nu}{d\mu}$.

Suppose $X = [a, b]$ and μ is the normalized Lebesgue measure on X. Let $\mathcal{X}$ be a random variable taking values in the space X with a probability density function f.

[1] A measure μ is σ-finite on X if X is a countable union of sets of finite μ-measure.

Then the probability that $\mathcal{X} \in A$ defines an absolutely continuous measure, namely

$$Prob\{\mathcal{X} \in A\} = \int_A f d\mu.$$

The following definition describes the typical transformation that will be encountered in this thesis.

Definition 2.8 *A transformation $S: X \to X$ is* **nonsingular** *if it is measurable and*

$$\mu(S^{-1}(A)) = 0$$

for all $A \in \mathcal{B}$ such that $\mu(A) = 0$.

Given a nonsingular transformation $S : X \to X$, we would like to obtain the probability density function of $S(\mathcal{X})$ in terms of that of $\mathcal{X}$. To do so, observe that

$$Prob\{S(\mathcal{X}) \in A\} = Prob\{\mathcal{X} \in S^{-1}(A))\} = \int_{S^{-1}(A)} f d\mu$$

Note that $\nu(A) = \int_{S^{-1}(A)} f d\mu$ defines an absolutely continuous measure since S is nonsingular. So by Theorem 2.7 there exists a ϕ such that

$$\nu(A) = \int_{S^{-1}(A)} f d\mu = \int_A \phi \, d\mu.$$

Thus ϕ is the probability density function of $S(\mathcal{X})$. This motivates the following definition.

Definition 2.9 (*The Perron-Frobenius operator*) *Let $S: X \to X$ be a nonsingular transformation. The* **Perron-Frobenius operator** *$\mathcal{L}: L^1_+ \to L^1_+$ corresponding to S is defined by*

$$\int_A \mathcal{L}f(x)\, \mu(dx) = \int_{S^{-1}(A)} f(x)\, \mu(dx) \tag{2.1}$$

for $A \in \mathcal{B}$, for any $f \geq 0$, $f \in L^1_+$.

The Perron-Frobenius operator maps the set of nonnegative L^1 functions into itself and preserves the L^1 norm (i.e. it is a Markov operator). These properties, among others, will prove to be very useful in studying the evolution of densities under a given transformation S. The operator $\mathcal{L}$ can be extended to all $f \in L^1$ by linearity. Namely, if g and h are nonnegative L^1 functions such that $f = g - h$, then

$$\mathcal{L}f = \mathcal{L}g - \mathcal{L}h.$$

Lemma 2.10 *The Perron-Frobenius operator $\mathcal{L}$ admits a unique extension to all of L^1.*

Proof. Firstly, notice that the operator $\mathcal{L}$ is linear on L^1_+. Let $f \in L^1$. Suppose $g, h, \bar{g}, \bar{h} \in L^1_+$ are such that $f = g - h = \bar{g} - \bar{h}$ (one such decomposition is $f = f^+ - f^-$, where $f^+ = \max_{x \in X}\{f, 0\}$ and $f^- = \max_{x \in X}\{-f, 0\}$). Then $\mathcal{L}f = \mathcal{L}g - \mathcal{L}h$, and we will show that $\mathcal{L}g - \mathcal{L}h = \mathcal{L}\bar{g} - \mathcal{L}\bar{h}$.

$$\begin{aligned}
g - h &= \bar{g} - \bar{h} \\
\Leftrightarrow g + \bar{h} &= h + \bar{g} \\
\Rightarrow \mathcal{L}(g + \bar{h}) &= \mathcal{L}(h + \bar{g}) \\
\Leftrightarrow \mathcal{L}g + \mathcal{L}\bar{h} &= \mathcal{L}h + \mathcal{L}\bar{g} \qquad \text{since } \mathcal{L} \text{ is linear on } L^1_+ \\
\Leftrightarrow \mathcal{L}g - \mathcal{L}h &= \mathcal{L}\bar{g} - \mathcal{L}\bar{h}.
\end{aligned}$$

Now, if $f = g - h$ define $\mathcal{L}f = \mathcal{L}g - \mathcal{L}h$. This yields a well defined operator on L^1, that is the unique extension of $\mathcal{L}$. □

We now make some important observations.

REMARKS:

i) Given f_1 and f_2 integrable functions such that

$$\int_A f_1(x)\,\mu(dx) = \int_A f_2(x)\,\mu(dx) \text{ for all } A \in \mathcal{B}$$

then $f_1 = f_2$ a.e. and since S is nonsingular, (2.1) uniquely defines $\mathcal{L}$ as an operator from L^1 to L^1.

ii) Suppose $X = [0,1] \subset \mathbb{R}$ and S is piecewise differentiable and invertible (in particular S is piecewise monotone). If A in Definition 2.1 is in fact an interval $[a,x]$, then a more explicit form of the operator $\mathcal{L}$ can be obtained. Suppose the intervals of monotonicity of S are B_α, such that for each α, $S_\alpha = S\Big|_{B_\alpha}$ is a one-to-one transformation with inverse S_α^{-1} and derivative $S'_\alpha \neq 0$. Let η denote the partition $\{B_\alpha\}$ of X. Differentiating both sides of (2.1) gives

$$\mathcal{L}f(x) = \frac{d}{dx} \sum_{\{\alpha:\, B_\alpha \in \eta\}} \int_{S_\alpha^{-1}([a,x])} f(s)\, ds \qquad \text{a.e.} \tag{2.2}$$

and a change of variables results in

$$\mathcal{L}f(x) = \sum_{\{\alpha:\, B_\alpha \in \xi\}} \frac{f(S_\alpha^{-1}(x))}{|S'(S_\alpha^{-1}(x))|} \chi_{S(B_\alpha)}(x). \tag{2.3}$$

Thus we have derived a pointwise formula for $\mathcal{L}$.

In order to clarify some of these ideas, it is instructive to consider the dyadic transformation on the unit interval with μ = Lebesgue measure. This example is presented next.

EXAMPLE 4: Let $S(x) = 2x(\text{mod } 1)$. To determine the Perron-Frobenius operator associated with the transformation S let $[0,x] \subset [0,1]$. Then $S^{-1}([0,x]) = [0,x/2] \cup [1/2, 1/2 + x/2]$ as shown in Figure 2.1. Hence by (2.2)

$$\mathcal{L}f(x) = \frac{d}{dx}\left(\int_0^{x/2} f(s)\, ds + \int_{1/2}^{1/2+x/2} f(s)\, ds\right) = \frac{1}{2}\left[f\left(\frac{x}{2}\right) + f\left(\frac{1}{2} + \frac{x}{2}\right)\right].$$

Definition 2.11 *A* **fixed point** *or an* **invariant function** *for an operator* $\mathcal{L} : L^1(X) \to L^1(X)$ *is a function* $f \in L^1(X)$ *with* $f \neq 0$ *and* $\mathcal{L}f = f$ μ*-a.e..*

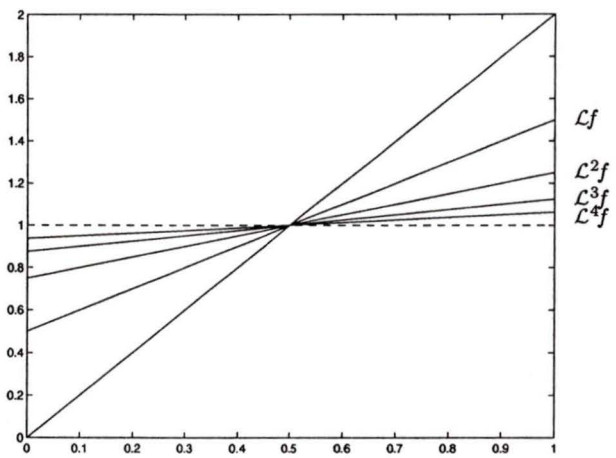

Figure 2.2: Illustrated are the first few iterates of the Perron-Frobenius operator with an initial density of $f_0(x) = 2x$. In this case $\mathcal{L}^n(f_0(x)) = 1 + (2x - 1)/2^n$, $n = 0, 1, \ldots$. The iterates converge rapidly to the invariant density $f_* = 1$.

It is easy to see that $f_* \equiv 1$ is a fixed point of the operator $\mathcal{L}$ corresponding to the dyadic transformation (i.e. $\mathcal{L}(1) = 1$).

Note that the probability density function f for the random variable $\mathcal{X}$ is a fixed point for the operator $\mathcal{L}$ if and only if $\mathcal{X}$ and $S(\mathcal{X})$ are equidistributed. The Perron-Frobenius operator may be viewed as the effect of the transformation S on a given probability density function.

Hence, by definition, if ν is an absolutely continuous invariant probability measure[2] for the transformation S then $f = d\nu/d\mu$ is an **invariant density function** corresponding to S, i.e. $f \geq 0$, $\int f d\mu = 1$ and $\mathcal{L}f = f$, μ−a.e..

To illustrate this concept, consider Example 4, and suppose that the initial density function is given by $f_0(x) = 2x$, where $x \in [0, 1]$. Then $\mathcal{L}(f_0(x)) = 1/2 + x$, and as can be seen in Figure 2.2, f will be rapidly flattened by the iterative application of the Perron-Frobenius operator. As $n \to \infty$, the density $\mathcal{L}^n(f_0(x)) =$

[2] ν is a probability measure on X if $\nu(X) = 1$.

$1-(2x-1)/2^n$ approaches the fixed point of $\mathcal{L}$, $f_*(x) \equiv 1$, $x \in [0,1]$.

Further study and applications of the Perron-Frobenius operator will be developed in Chapter 3.

Suppose S is measurable and $E \in \mathcal{B}$. For $x \in X$ we may be interested in the frequency with which the points of the orbit $\{x, Sx, S^2x, \ldots\}$ occur in the set E. The next theorem addresses this issue and is an important result due to G. D. Birkhoff proved in 1931.

Theorem 2.12 *(Birkhoff Ergodic Theorem) Let $(X, \mathcal{B}, \nu)$ be a σ-finite measure space. Let $S : (X, \mathcal{B}, \nu) \to (X, \mathcal{B}, \nu)$ be measure preserving and $f \in L^1(\nu)$. Then there exists a function $f^* \in L^1(\nu)$ such that*

$$\lim_{n\to\infty} A_n(f) = \lim_{n\to\infty} \frac{1}{n} \sum_{k=0}^{n-1} f(S^k(x)) = f^*, \qquad \nu - a.e..$$

Furthermore, f^* is invariant, i.e. $f^* \circ S = f^*$, $\nu-a.e.$ and if $\nu(X) < \infty$, then

$$\int_X f^* d\nu = \int_X f d\nu.$$

Proof. See Góra [9]. □

Let us apply this theorem to $f = \chi_E$. Observe that $\chi_E(S^k x) = 1$ if $S^k x \in E$ and zero otherwise. Therefore,

$$A_n(\chi_E)(x) = \frac{1}{n} \sum_{k=0}^{n-1} \chi_E(S^k x)$$

gives the relative frequency that the finite orbit $\{x, Sx, \ldots, S^{n-1}x\}$ meets E. Thus Birkhoff's Theorem implies that for a.e. (ν) x, the limiting frequency exists and

$$\lim_{n\to\infty} A_n(\chi_E)(x) = \chi_E^*(x).$$

That is, the limiting relative frequency of visits to the target set E by the orbit starting at x exists, but depends on x. The Birkhoff theorem gives two implications

about this dependence. Firstly, the invariance of χ_E^* implies that two points on the same orbit give rise to the same frequency (obvious if one assumes that the limiting frequency exists). The second implication is that $\int_X \chi_E(x)\, d\nu(x) = \nu(E)$, meaning that the expected, or average frequency of visits to target set E is the measure of E (although it is possible that no orbits yield this average frequency, as will be shown later). In general not much more can be said about the function χ_E^*. However for *ergodic transformations* S defined below the function χ_E^* has a particularly simple form.

Firstly we need the notion of invariant sets under a given transformation.

Definition 2.13 *Let $S : (X, \mathcal{B}, \mu) \to (X, \mathcal{B}, \mu)$ be measure preserving. A set A is called an* **invariant set** *under S if $S^{-1}(A) = A$.*

Definition 2.14 *Let $S : (X, \mathcal{B}, \mu) \to (X, \mathcal{B}, \mu)$ be measure preserving. If any invariant set $A \in \mathcal{B}$ is such that either $\mu(A) = 0$ or $\mu(X/A) = 0$ then S is called* **ergodic**.

That is, S is ergodic if the only invariant sets are trivial sets. Equivalently, the space X may not be decomposed into two nontrivial invariant sets, $X = A \cup X \backslash A$ with $\mu(A) \neq 0$ and $\mu(X \backslash A) \neq 0$.

The next Lemma gives an equivalent but more convenient condition for checking ergodicity.

Definition 2.15 *The* **symmetric differnce** *of sets A and B is defined by*

$$A \triangle B = (A \backslash B) \cup (B \backslash A).$$

Lemma 2.16 *Let $S : X \to X$ be a measure preserving transformation. Then S is ergodic if and only if the only members $B \in \mathcal{B}$ with $\mu(S^{-1}B \triangle B) = 0$ are such that $\mu(B) = 0$ or $\mu(X)$.*

Proof. ($\Leftarrow$) Let S be a measure preserving transformation such that $\mu(S^{-1}B \triangle B) = 0$ only if $\mu(B) = 0$ or 1. Thus the only invariant sets are the trivial sets.

($\Rightarrow$) Let S be ergodic and suppose $B \in \mathcal{B}$ with $\mu(S^{-1}B \triangle B) = 0$. We need to show $\mu(B) = 0$ or 1. We shall do so by constructing a set B_∞ which has the same measure as B and is invariant under S. Observe that $S^{-n}B \triangle B \subset \bigcup_{i=0}^{n-1} S^{-(i+1)}B \triangle S^{-i}B = \bigcup_{i=0}^{n-1} S^{-i}(S^{-1}B \triangle B)$, and hence $\mu(S^{-n}B \triangle B) \leq n\mu(S^{-1}B \triangle B)$. Thus for each $n > 0$, $\mu(S^{-n}B \triangle B) = 0$. Define B_∞ by

$$B_\infty = \bigcap_{n=0}^{\infty} \bigcup_{i=n}^{\infty} S^{-i}B. \tag{2.4}$$

By our previous computation, for each $n \geq 0$ we have

$$\mu(B \triangle \bigcup_{i=n}^{\infty} S^{-i}B) \leq \sum_{i=n}^{\infty} \mu(B \triangle S^{-i}B) = 0.$$

Since the sets $\bigcup_{i=n}^{\infty} S^{-i}B$ decrease with n and each has measure equal to B, we have $\mu(B_\infty \triangle B) = 0$, thus $\mu(B_\infty) = \mu(B)$. To show that B_∞ is also invariant, we compute $S^{-1}B_\infty$ using Definition 2.4.

$$S^{-1}B_\infty = \bigcap_{n=0}^{\infty} \bigcup_{i=n}^{\infty} S^{-(i+1)}B = \bigcap_{n=0}^{\infty} \bigcup_{i=n+1}^{\infty} S^{-i}B = B_\infty.$$

Thus $\mu(B_\infty) = \mu(B) = 0$ or 1. □

It is often quite difficult to determine directly from Definition 2.14 if a given measure preserving map is ergodic. However, in the next example we prove the ergodicity of the dyadic map introduced in Example 2.

EXAMPLE 5: Let $S(x) = 2x(\text{mod } 1)$, $\mathcal{B}$ = Borel σ-algebra of $[0,1)$ and μ = Lebesgue measure on $[0,1)$. To show that S is ergodic consider $A = S^{-1}(A)$. We will prove that $\mu(A)$ equals either 0 or 1. This will be done in steps. In Step 1 we will prove that $\mu(A \cap [0,1/2)) = \mu(A)\mu([0,1/2))$. In Step 2 we prove this for the intersection $A \cap E$, where E is a subinterval of $[0,1)$ with dyadic endpoints. In Step 3 we extend

this result to a union of dyadic intervals, subsequently proving the result within ϵ for $A \cap A$. From this we will conclude that $\mu(A)$ must be either 0 or 1.

Step 1: Let $S_1 : [0,1/2) \to [0,1)$ and $S_2 : [1/2,1) \to [0,1)$ denote the transformation S restricted to the intervals $[0,1/2)$ and $[1/2,1)$ respectively. Observe that for all $y \in [0,1)$, $S_1^{-1}(y) = S^{-1}(y) \cap [0,1/2)$, while $S_2^{-1}(y) = S^{-1}(y) \cap [1/2,1) = S_1^{-1}(y) + 1/2$. Then

$$\begin{aligned}
\mu(A \cap [1/2,1)) &= \mu(S^{-1}A \cap [1/2,1)) \qquad \text{(since } A = S^{-1}A\text{)} \\
&= \mu(S_2^{-1}A) \\
&= \mu(S_1^{-1}A + 1/2) \\
&= \mu(S_1^{-1}A) \qquad \text{(since } \mu \text{ is translation invariant)} \\
&= \mu(S^{-1}A \cap [0,1/2)) \\
&= \mu(A \cap [0,1/2))
\end{aligned}$$

Thus for $I = [0,1)$

$$\mu(A) = \mu(A \cap S^{-1}I) = 2\mu(A \cap S_1^{-1}I) = 2\mu(A \cap S_2^{-1}I). \tag{2.5}$$

Step 2: If E is an interval of the form

$$E = \left[\frac{s}{2^{k+1}}, \frac{s+1}{2^{k+1}}\right)$$

where k is a nonnegative integer and $s = 0, 1, \ldots, 2^{k+1} - 1$, then

$$\mu(A \cap E) = \mu(A)\mu(E). \tag{2.6}$$

This is shown by induction. The basis step is expression (2.5). Assume that (2.6) holds for $k = m$ and $s = 0, 1, \ldots, 2^{m+1} - 1$. We need to show that the statement is true for $E = [s/2^{m+2}, (s+1)/2^{m+2})$. Notice that E is entirely contained in either $[0,1/2)$ or $[1/2,1)$, that is $E \cap [0,1/2) = E$ or $\emptyset$. Without loss of generality suppose

$E \cap [0, 1/2) = E$. Then using (2.5) with $S_1^{-1} I = E$ and the induction hypothesis we obtain

$$\begin{aligned}
\mu(A \cap E) &= \mu(A \cap S_1^{-1} I) \\
&= \frac{1}{2}\mu(A \cap S^{-1} I) \qquad \text{(follows from expression 2.5)} \\
&= \frac{1}{2}\mu(S^{-1}(A \cap I)) \\
&= \frac{1}{2}\mu(A \cap I) \\
&= \frac{1}{2}\mu(A)\,\mu\left(\left[\frac{s}{2^{m+1}}, \frac{(s+1)}{2^{m+1}}\right)\right) \qquad \text{(by Induction Hypothesis)} \\
&= \mu(A)\,\mu\left(\left[\frac{s}{2^{m+2}}, \frac{(s+1)}{2^{m+2}}\right)\right) \\
&= \mu(A)\mu(E).
\end{aligned}$$

Step 3: The result of Step 2 can be extended to any set which is a finite union of dyadic intervals.

Let $E = \bigcup_{j=1}^{n} E_j$ be a finite union of dyadic intervals. Without loss of generality we can assume the E_j are disjoint and so

$$\begin{aligned}
\mu(A \cap \bigcup_{j=1}^{n} E_j) &= \mu(\bigcup_{j=1}^{n} (A \cap E_j)) \\
&= \sum_{j=1}^{n} \mu(A \cap E_j) \\
&= \sum_{j=1}^{n} \mu(A)\mu(E_j) \\
&= \mu(A)\mu(E).
\end{aligned}$$

Consider $\epsilon > 0$. The set A can be approximated arbitrarily closely by a union of dyadic intervals $B = \bigcup_{i=1}^{n} E_i$ such that $\mu(A \triangle B) = \mu((A - B) \cup (B - A)) \leq \epsilon/2$. Therefore

$$\mu(A)(1 - \mu(A)) \leq \mu(A)\left(1 - \mu(B) + \frac{\epsilon}{2}\right)$$

$$\begin{aligned} &= \mu(A) - \mu(A)\mu(B) + \frac{\epsilon}{2}\mu(A) \\ &= \mu(A) - \mu(A \cap B) + \frac{\epsilon}{2}\mu(A) \\ &\leq \mu(A) - \left(\mu(A) - \frac{\epsilon}{2}\right) + \frac{\epsilon}{2} \\ &= \epsilon. \end{aligned}$$

Since ϵ was chosen arbitrary this implies $\mu(A) = 0$ or $\mu(A) = 1$. Hence the dyadic map is ergodic.

The following theorem gives an important characterization of ergodic maps.

Theorem 2.17 *The following are equivalent*

1. *S is ergodic.*
2. *If f is measurable and $f \circ S = f$ a.e., then f is constant a.e.*

Proof. ($\Rightarrow$) Suppose S is ergodic and let f be such that $f \circ S = f$ a.e.. If f is not constant a.e., then there exists $a \in \mathbb{R}$ such that the set $B = \{x | f(x) \leq a\}$ is a nontrivial set. We will show that $B = S^{-1}B$, thus contradicting the ergodicity of S.

Let $x \in S^{-1}B$. Then $S(x) \in B$, and $f(S(x)) = f(x) \leq a$. Thus $x \in B$.

Let $x \in B$. Then $f(x) \leq a$, thus $f(S(x)) \leq a$, or $S(x) \in B$. Therefore $x \in S^{-1}B$ and $B = S^{-1}B$.

($\Leftarrow$) Suppose for all measurable functions f with the property $f \circ S(x) = f(x)$ we have that f is constant a.e.. Let B be a set in X with the property $S^{-1}B = B$. Consider the characteristic function on B, χ_B. Since B is invariant $\chi_B(S(x)) = \chi_B(x) = 1$ on B and zero otherwise. Hence $\chi_B \circ S(x) = \chi_B(x)$ and by assumption χ_B is constant a.e.. Thus $\mu(B) = 0$ or $\mu(X \backslash B) = 0$, which proves that S is ergodic. □

The next corollary follows directly from Theorem 2.12 and Theorem 2.17.

Corollary 2.18 *If S is ergodic then the invariant function f^* is constant $\nu-$a.e.*

and if $\nu(X) < \infty$, *then*

$$f^* = \frac{1}{\nu(X)} \int_X f \, d\nu, \qquad \nu - a.e..$$

Returning to the calculation of the frequency of visits of an orbit $\{x, Sx, S^2x, \ldots\}$ to a measurable set E, it follows from Theorem 2.17 that if S is ergodic then

$$\chi_E^* = \nu(E) \qquad \text{a.e..}$$

That is, the orbit of almost every point of X occurs in the set E with asymptotic frequency $\nu(E)$.

The following outlines a method for computing an estimate for the invariant density function given an ergodic transformation $S : X \to X$, where $X = [0, 1)$.

Let $\nu = f \, d\mu$ be invariant. For each subset $E \in X$ and for a.e. $x \in X$ we have

$$A_n \chi_E(x) \to \nu(E) = \int_E f \, d\mu.$$

If E is a short interval $E = (a, b)$, then

$$\int_E f \, d\mu = \left(\frac{1}{b-a} \int_a^b f \, d\mu \right) (b - a) = \bar{f}_{(a,b)} \mu(a, b)$$

where $\bar{f}_{(a,b)}$ denotes the average value of density f on (a, b). This motivates partitioning the space X into intervals.

Definition 2.19 *An* **n-bin partition** η *of* $X = [0, 1)$ *is a finite set* $\{x_0, x_1, \ldots, x_n\}$ *of real numbers such that*

$$0 = x_1 < x_2 < x_3 < \cdots < x_n < 1.$$

The intervals $[x_i, x_{i+1})$ *for* $i = 1, \ldots, n-1$ *are called the* **component intervals** *or* **bins** *of the partition* η. *If the component intervals have the same measure, i.e.* $\mu([x_i, x_{i+1})) = 1/n$ *for all* $i = 1, \ldots, n-1$, *then we say that* η *is a* **uniform partition** *of* X *with* $|\eta| = 1/n$.

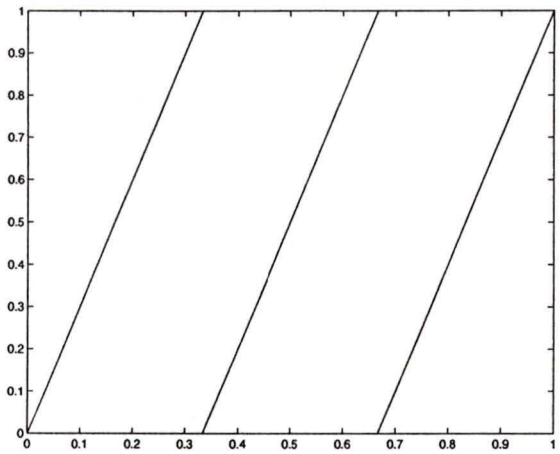

Figure 2.3: The transformation $S(x) = 3x(\text{mod } 1)$ on $[0, 1]$.

In the next two examples we will use a uniform fifty-bin partition η to obtain a picture of $f \approx \sum_{I \in \eta} \bar{f}_I \chi_I$ by calculating

$$\bar{f}_I = \lim_{n \to \infty} \frac{A_n \chi_I(x)}{|\eta|} = 50 \lim_{n \to \infty} A_n \chi_I(x).$$

The examples will show that for some values of x this gives an approximation for the true invariant density function, while others fall in the exceptional set of Birkhoff's Theorem, and produce incorrect estimates.

To illustrate how we can make an estimate for the invariant measure for a given transformation S consider the following two situations illustrated by the next example.

EXAMPLE 6: Let $S(x) = 3x(\text{mod } 1)$ and refer to Figure 2.3. Let η be the partition of $[0, 1]$ into 50 equal sized bins. For each $E \in \eta$ we may obtain an approximation for the measure $\nu(E)$ using the Birkhoff Ergodic Theorem with

$$\nu(E) \approx \nu_{(n,x_0)}(E) = A_n(\chi_E) = \frac{\#\{i < n : S^i(x_0) \in E\}}{n}$$

where $\#C$ denotes the number of elements in the set C. For any given initial point x_0, $\nu_{(n,x_0)}(E)$ represents the fraction of hits which occur in the set E. In particular

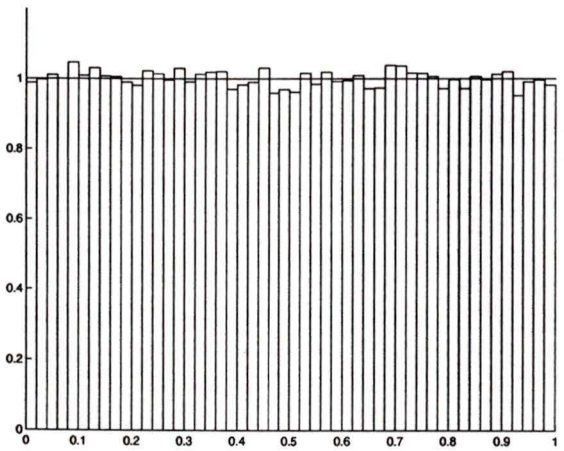

Figure 2.4: The estimate for the density of ν for $S(x) = 3x(\text{mod } 1)$. The orbit has a length of $n = 10^5$ and starts at $x = \sqrt{2}/2$.

we may think of $\{\nu_{(n,x_0)}(E)\}_{n=1}^{\infty}$ as a sequence of measures which converges weakly to an invariant density function on E. Consider the orbit of the initial point $x = \sqrt{2}/2$. Computer simulations for an orbit of length $n = 10^5$ produce the estimate for the invariant density shown in Figure 2.4.

In contrast, consider the orbit of the initial point $x = 1/3$. By observing that $S(1/3) = 0$ and subsequently $S^i(0) = 0\ \forall i \geq 1$, we see that in this case

$$\nu(E) = \lim_{n\to\infty} \nu_{(n,1/3)}(E) = \begin{cases} 1 & \text{if } 0 \in E \\ 0 & \text{if } 0 \notin E. \end{cases}$$

Therefore the orbit of the exceptional point $x = 1/3$ produces a δ-function peaked at zero in the limit as $n \to \infty$. Computer simulations verify this result, which is illustrated in Figure 2.5.

Example 6 shows the sensitivity to the choice of the starting point on the resulting invariant density. Starting at $x = \sqrt{2}/2$ produced an estimate for the true invariant density $f = 1$, while starting at $x = 1/3$ produced a δ-function. Clearly this latter density is the incorrect invariant density for the triadic map.

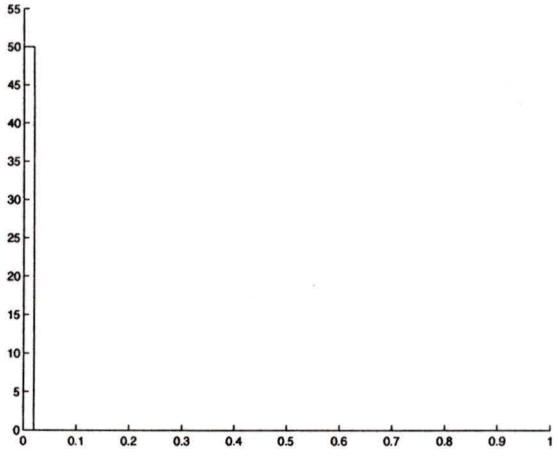

Figure 2.5: The estimate for the density of ν with an orbit of length $n = 10^5$ of $S(x) = 3x(\text{mod } 1)$ with an initial point $x = 1/3$. This approximates the δ-function at $x = 0$.

The next example shows that the exceptional set of initial points x in Birkhoff's Theorem can nontheless be troublesome in applications. Recall that every number in a computer is represented by a dyadic rational, in any precision.

EXAMPLE 7: Let $S(x) = 2x(\text{mod } 1)$ and let the partition η be as above. Then apply the Birkhoff theorem as in the above example to the orbit corresponding to initial point $x = 1/2^n$ for some positive integer n. It is easy to see that $S^n(x) = 0$. In fact because of its floating point representation, every starting point $x \in [0, 1]$ for this transformation will produce a δ-function as shown in Figure 2.5.

2.3 Conclusion

Although intuitive, the Birkhoff ergodic method of computing the invariant density function has a number of drawbacks. This method is based on the assumption that the map of interest is ergodic. We illustrated that even in the dyadic example, one which is relatively simple from the point of view of computations, ergodicity is dif-

ficult to prove. The map of main interest in this thesis will be derived numerically using an approximation scheme. This makes ergodicity difficult or impossible to prove. In addition, computing long orbits using the approximation scheme compounds on the round off error and makes the invariant density estimate less reliable.

Another drawback to this method is that, as illustrated in the dyadic and triadic examples, it is highly dependent on the choice of orbits. In particular, certain initial orbit points belong to the exceptional set (of measure zero) which do not produce the correct invariant density function. In addition, due to some limitations of the floating point representations language, it is possible that all points produce an incorrect invariant density function (as shown in the dyadic example). The numerics require long orbits and laborious computations, which make this method also time inefficient. Furthermore, the rate of convergence to the invariant density function is unknown and there are no error estimates that can be made. In this thesis we will develop a method that will address some of these issues.

Chapter 3

Invariant Density Function for the Rock Drill Map

3.1 Introduction

In this chapter a 2-dimensional rock drill model will be presented based on the geometry and the linear speed of the individual wheel of the drill. This was a model first presented by Lasota and Rusek [8] in 1974. In their analysis an estimate for the invariant measure was obtained using the method outlined in Chapter 2. This estimate is the objective of this chapter. In Section 3.2 we will see that the behaviour of the drill is directly related to the Froude number, dependent on the linear speed of the drill's wheel and the force exerted by the drill onto the rock. Important conditions on this ratio will be discussed and we will see how one can numerically obtain a map which will fully describe the behaviour of the drill for different speeds. Motivated by the results for unit interval transformations in ergodic theory, in Section 3.3 the drill map will be redefined from the unit interval into itself. This map will be our main focus throughout the remainder of the thesis, in particular we will be interested in computing its invariant density function, given that it exists. In order to apply the existence result of Lasota-Yorke on absolutely continuous invariant measures, in Section 3.4 the idea of induced mappings is presented and

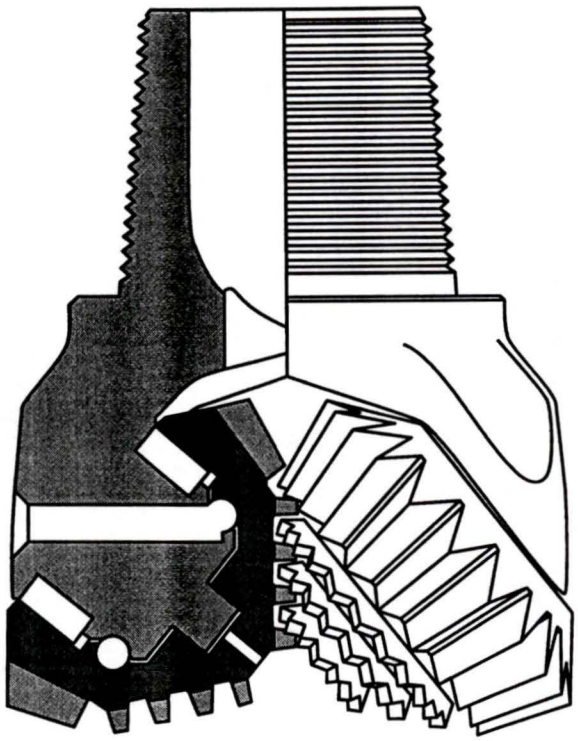

Figure 3.1: Illustrated above is a rock drill bit with three conical cutting heads.

applied to the rock drill transformation. In Section 3.5 we use the existence of an absolutely continuous invariant measure to apply the Birkhoff Ergodic Theorem presented in Chapter 2 and obtain an estimate for the invariant density function of the rock drill map.

3.2 Rock Drill Model

A rock drill consists of a number of intermeshed toothed wheels as illustrated in Figure 3.1. The drill bit rotates about its central axis, and each wheel rotates about its centre.

In this thesis the model is based on the action of only one of the wheels of the drill. This makes the model two-dimensional, with one dimension being the

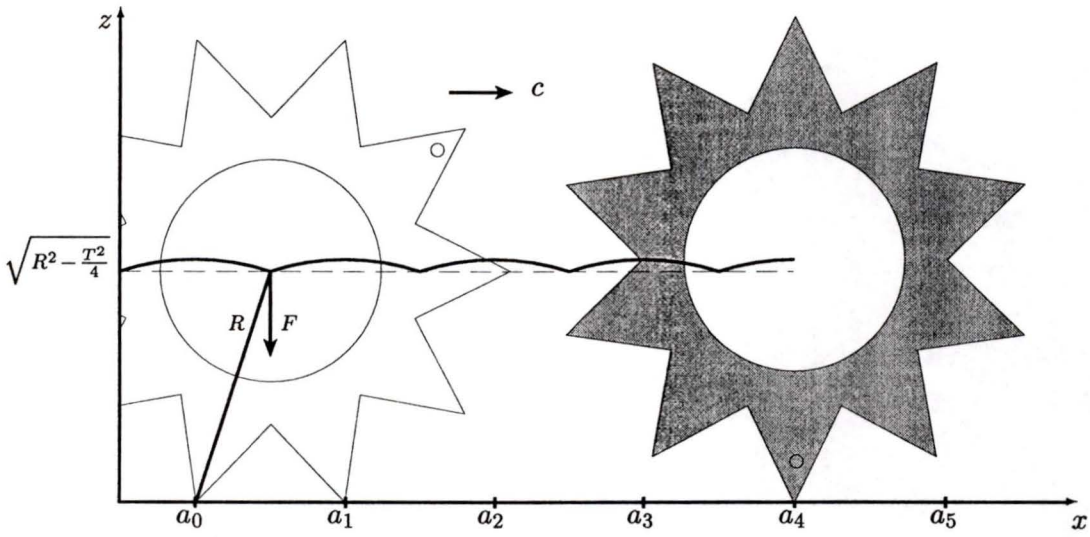

Figure 3.2: The cutting head is comprised of a number of gears. Illustrated is one such gear and the curve $q(x)$ mapped out by its centre when the gear rolls.

horizontal travel of the wheel and the other dimension describing vertical motion of the wheel hitting the rock. Let R be the radius of the wheel and T be the straight line distance between two consecutive teeth. Then the curve described by the centre of the wheel is periodic with period T, and consists of segments of circles of radius R and centres $a_k = (2k+1)T/2$ for $k = 0, 1, \ldots$. Namely $q(x) = \sqrt{R^2 - (x - a_k)^2}$ for $kT \leq x \leq (k+1)T$. This is shown in Figure 3.2. Then

$$f_k(x) = \sqrt{R^2 - \left[x - T\left(k + \frac{1}{2}\right)\right]^2} - \sqrt{R^2 - \frac{T^2}{4}}$$

for $kT \leq x \leq (k+1)T$ is the $(k+1)$-th hump described by the centre of the wheel after the curve has been shifted down to the x-axis. We define the base curve $f(x)$ with domain $x \geq 0$ to be $f(x) = \sum_{k=0}^{\infty} f_k(x)\chi_{[kT,(k+1)T)}(x)$[1].

[1] χ_B is the characteristic function on the set B, defined by

$$\chi_B(x) = \begin{cases} 0 & : \quad x \notin B \\ 1 & : \quad x \in B \end{cases}$$

The centre of the wheel describes the curve $f(x)$ if the component of the net reaction force on the wheel in the direction normal to the base curve points towards the rock surface. Thus, in this case the vertical component $\mathcal{F}_z$ of the net reaction force must be negative.

Let F be the applied vertical force on the drill (i.e. the weight of the drill plus the press force), and M be the mass of the drill. We use Newton's Law to make an estimate on the drill's parameters in the case when the wheel simply rolls along the rock. Let c be the x component of the velocity of the mass centre of the wheel and t be time. Then $x = ct$ and

$$\mathcal{F}_z = -M\frac{d^2\hat{f}}{dt^2} - F$$

where $\hat{f}(t)$ is the curve described by the centre of the wheel as a function of time. For $kT \leq x \leq (k+1)T$

$$\frac{d^2\hat{f}}{dt^2} = c^2\frac{d^2f}{dx^2} = -\frac{c^2R^2}{(q(x))^3}$$

where $q(x) = f(x) + \sqrt{R^2 - T^2/4}$ for all x. Thus for $\mathcal{F}_z < 0$ we need

$$\begin{aligned}
\mathcal{F}_z &= Mc^2\frac{R^2}{(q(x))^3} - F < 0 \\
&\Leftrightarrow F\left(1 - \frac{Mc^2R^2}{F(q(x))^3}\right) > 0 \\
&\Leftrightarrow F\left(1 - \omega^2\frac{R^3}{(q(x))^3}\right) > 0
\end{aligned}$$

where $\omega^2 = \frac{Mc^2}{FR}$ is known as the Froude number and represents the ratio between the force due to the rotation of the wheel, Mc^2/R, and the applied force, F, exerted by and on the drill. In this thesis it will be assumed that the only applied vertical force is that due to gravity, namely $F = Mg$. Thus the Froude number simplifies to $\omega^2 = \frac{c^2}{gR}$. Notice that ω is proportional to c. The condition above translates to the inequality

$$\omega^2 < \frac{(q(x))^3}{R^3}$$

for all $x \in \mathbb{R}^+$. There are three cases.

Case 1:

$$0 \leq \omega^2 \leq \min_{x \in \mathbb{R}^+} \left(\frac{(q(x))^3}{R^3} \right).$$

The quantity $(q(x))^3/R^3$ is minimum when $q(x)$ is minimum, namely when $x = kT$, $k = 0, 1, 2, \ldots$. Substituting $q(kT) = q(0) = \sqrt{R^2 - T^2/4}$ gives the condition on ω^2

$$0 \leq \omega^2 \leq \frac{(q(kT))^3}{R^3} = \left(1 - \frac{T^2}{4R^2} \right)^{3/2}.$$

In this case at least one tooth of the wheel is in contact with the rock at all times. That is, the linear speed is low and the wheel simply rolls along the surface of the rock.

Case 2:

$$\min_{x \in \mathbb{R}^+} \left(\frac{(q(x))^3}{R^3} \right) < \omega^2 < \max_{x \in \mathbb{R}^+} \left(\frac{(q(x))^3}{R^3} \right).$$

The ratio $(q(x))^3/R^3$ attains its maximum when $q(x)$ is maximum, which occurs at a_k. The substitution $q(a_k) = R$ gives the condition

$$\frac{(q(kT))^3}{R^3} = \left(1 - \frac{T^2}{4R^2} \right)^{3/2} < \omega^2 < \frac{(q(a_k))^3}{R^3} = 1.$$

In this case, the linear speed is sufficient for the wheel to bounce off the rock as long as the position of the centre of the wheel, x, is outside an interval, I_k, around $x = a_k$. In other words launching will occur over $\mathbb{R}^+ \backslash I_k$, otherwise the wheel rolls along the surface of the rock.

Case 3:

$$\omega^2 \geq 1.$$

In this case the linearl speed of the wheel is high enough, so that the drill always bounces off the rock at point of contact. This case will be our main interest in this thesis.

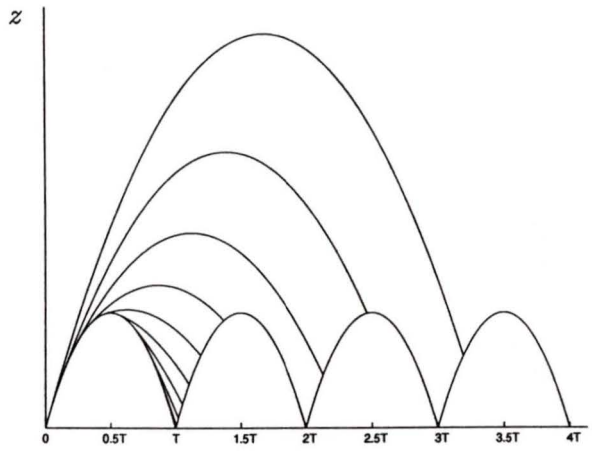

Figure 3.3: Projectile motion described by the centre of the drill head once it launches from the first base curve.

For effective drilling the linear speed of the wheel should be high enough so that the drill bit jumps away and subsequently lands back on the rock, hence transferring its kinetic energy into work (i.e. drilling). However $\omega^2 > 1$ does not ensure uniform drilling. When $1 < \omega^2 < 2$ the wheel's trajectory rapidly approaches a periodic regime in that the drill lands on the same position of the base curve on every jump. This will be briefly discussed later on.

We assume that there is no sliding of the teeth and all collisions are completely inelastic. Figure 3.2 shows what happens as the wheel jumps away from the rock. The centre describes a projectile motion curve which is initially tangential to the base curve (corresponding to the assumption of inelasticity, i.e. no sliding of the teeth in the x direction) and its range depends on the launch point and the linear speed of the wheel. We will be interested in studying a map which describes the orbit of any given initial launch point, thus enabling us to study the longtime average landing point distribution, that is the uniformity of impacts and rate of drilling. Because of

this we are interested in the map $L(x_0)$, i.e. landing point L vs. launch point x_0. Iterates of L will produce the orbit of a given initial point x_0. To find an explicit form of the function L assume $0 \leq x_0 \leq T$, i.e. launching occurs at $(x_0, f_0(x_0))$. Then the projectile motion curve $u(t) = (x(t), z(t))$ satisfies

$$\ddot{u}(t) = (0, -g) \tag{3.1}$$

with initial conditions

$$u(0) = (x_0, f_0(x_0)), \qquad \dot{u}(0) = (c, cf_0'(x_0)).$$

Simple integration of both sides of (3.1) and using the initial conditions leads to

$$u(t) = (ct + x_0, -\frac{gt^2}{2} + ctf_0'(x_0) + f_0(x_0)).$$

By letting $x = x_0 + ct$ be the horizontal position of the mass centre of the wheel one has

$$u(t) = (x, w(x, x_0)),$$

where

$$w(x, x_0) = f_0(x_0) + (x - x_0)f_0'(x_0) - \frac{g}{2c^2}(x - x_0)^2.$$

Note that $w(x, x_0)$ describes the orbit of the mass centre of the wheel as a function of the initial launch point. It will enable us to obtain the landing point L as a function of x_0. We do so by fixing x_0 and solving for L in

$$w(L, x_0) = f_k(L)$$

where k is the smallest integer satisfying this equation. Figure 3.4 shows $L(x_0)$ for a typical wheel ($R = 0.032$m, $T = 0.0198$m), when the linear velocity of the wheel is $c = 1.0\text{ms}^{-1}$. Here $\omega^2 = 3.186$. The graph of L is based on 10^5 points numerically determined using an approximation scheme similar to Newton's method (see Appendix A).

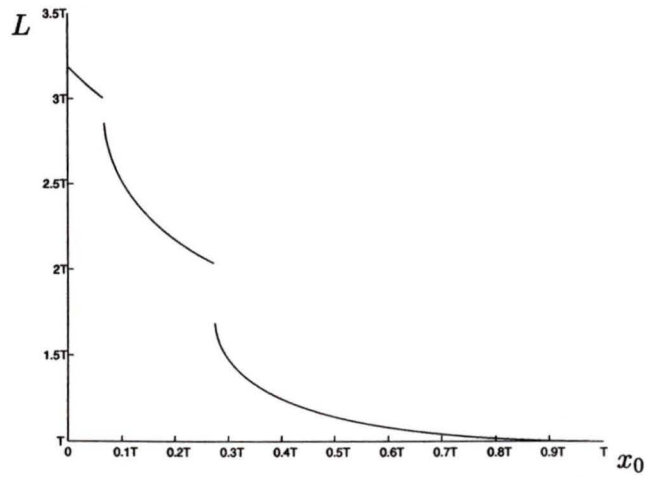

Figure 3.4: Depicted is the trajectory map $L(x_0)$ where $R = 3.2\text{cm}$, $T = 1.98\text{cm}$ (the wheel has 10 teeth) and $c = 1.0\text{ms}^{-1}$ ($\omega = 1.78$). With this set of parameters the trajectory map has three disjoint branches.

An important feature of the map L is its monotonicity. We prove in the next lemma that the map L is piecewise monotone decreasing provided the speed c is sufficiently large.

Lemma 3.1 *There exists a critical speed v_{crit} such that whenever $c > v_{crit}$ the map L is piecewise monotone decreasing.*

Proof. We show this by proving the monotonicity of $w(x, x_0)$ as a function of x_0 for a fixed x. Figure 3.5 shows this geometrically. We seek a condition for which $\partial w/\partial x_0 < 0$, where

$$w(x_0) = -\frac{g}{2c^2}(x - x_0)^2 + (x - x_0)f_0'(x_0) + f_0(x_0).$$

We need

$$\begin{aligned}\frac{\partial w}{\partial x_0} &= \frac{g}{c^2}(x - x_0) - f_0'(x_0) + (x - x_0)f_0''(x_0) + f_0'(x_0) \\ &= (x - x_0)\left(f_0''(x_0) + \frac{g}{c^2}\right) < 0.\end{aligned}$$

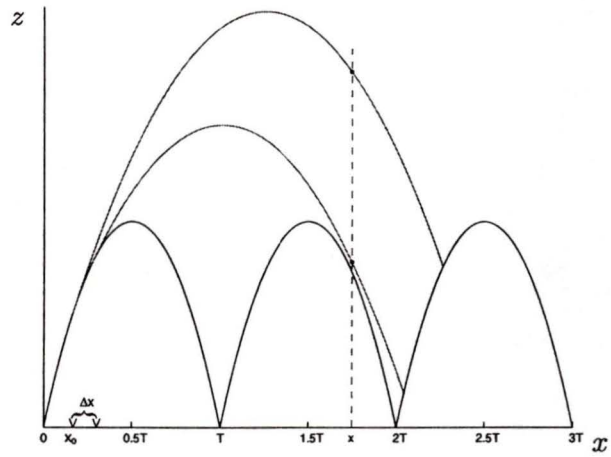

Figure 3.5: Depicted are two trajectories with launching points x_0 and $x_0 + \triangle x$ and parameters $R = 3.2\text{cm}$, $T = 1.98\text{cm}$ ($\gamma = 9.55 \times 10^{-2}$) and $c = 1.0\text{ms}^{-1}$ ($\omega = 1.78$). Geometry suggests $w(x, x_0 + \triangle x) < w(x, x_0)$.

Since $x > x_0$, one must have $c^2 > v_{crit}^2 = -g/f_0''(x_0)$.

For our base curve $f_0(x_0)$,

$$f_0''(x_0) = \frac{-R^2}{\left[R^2 - \left(x_0 - \frac{T}{2}\right)^2\right]^{3/2}} < 0$$

Therefore the maximum of $-g/f_0''(x_0)$ is attained when $x_0 = 0$. Hence the condition for the critical speed becomes

$$v_{crit}^2 = \frac{g}{R^2}\left(R^2 - \frac{T^2}{4}\right)^{3/2}. \quad \square$$

Applied to a typical wheel ($R = 3.2\text{cm}$ and $T = 1.98\text{cm}$) Lemma 3.1 gives the monotonicity condition $c \geq 0.27\text{ms}^{-1}$.

For further analysing the map L we wish to nondimensionalize its parameters, hence obtaining a base curve of period one. This is done by making the following

substitutions:

$$x = sT, \qquad p_k(s) = \frac{f_k(sT)}{R}.$$

Under this substitution the new form for the base curve becomes

$$p_k(s) = [1 - \gamma(2s - 2k - 1)^2]^{1/2} - (1 - \gamma)^{1/2}$$

where $k \leq s \leq k + 1$ and $\gamma = (T/2R)^2$ is a dimensionless parameter depending only on the number of teeth on the wheel[2]. Notice $p_k(s)$ corresponds to the k-th hump of the base curve. The new base curve $p(s)$ with domain $s \geq 0$ is defined to be $p(s) = \sum_{k \in \mathbb{N}} p_k(s)\chi_{[k,k+1]}(s)$. The map landing point Y vs. launch point s_0 may be obtained similarly as above. That is by solving for Y as a function of s_0 in

$$p(s_0) + (Y - s_0)p'(s_0) - \frac{2\gamma}{\omega^2}(Y - s_0)^2 = p(Y). \tag{3.2}$$

Furthermore the condition corresponding to the critical speed translates to

$$\omega^2 = (1 - \gamma)^{3/2}$$

and by Lemma 3.1 this is sufficient for the monotonicity of $Y(s)$.

3.3 Unit-Interval Map For The Rock Drill

Our interest in the map Y lies in determining where the drill hits the rock when it lands. Recall that the variable s represents how much the drill has turned. We may think of the unit interval applied N times around the circumference of the wheel, where N is the number of teeth on a wheel. We shall restrict our attention to the map $S : [0, 1] \to [0, 1]$ defined by

$$S(s) = Y(s) (\text{mod } 1).$$

[2] $\gamma = \sin^2(\pi/N)$, where N is the number of teeth on the wheel.

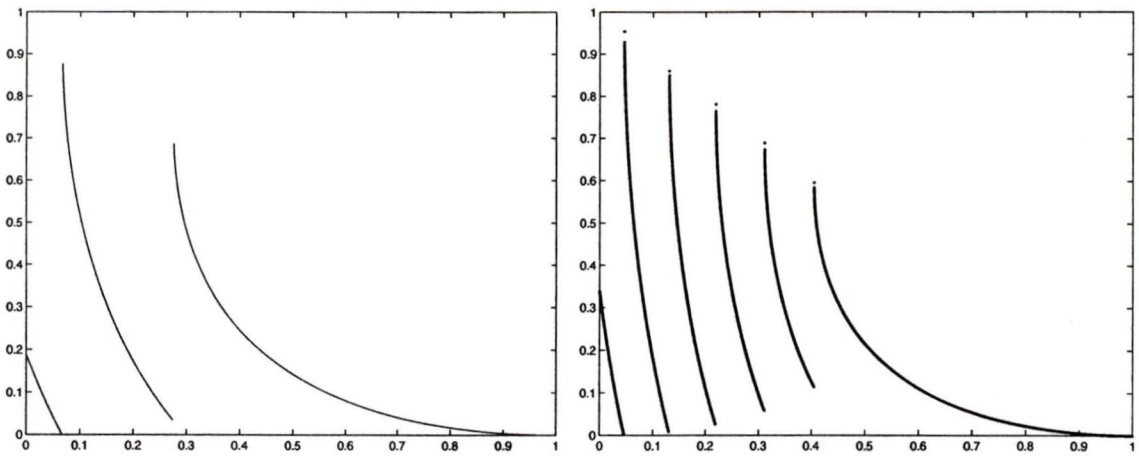

Figure 3.6: Left: Depicted is the unit-interval rock drill map $S : [0,1] \to [0,1]$ with $\gamma = 9.55 \times 10^{-2}$ and $\omega = 1.78$. Right: the unit-interval map $S : [0,1] \to [0,1]$ with same drill parameters and $\omega = 2.5$.

Figure 3.6 shows the unit interval map S corresponding to the behaviour of a drill with typical parameters and speeds of $c = 1.0$ m/s and $c = 1.4$ m/s.

The piecewise monotonicity of the map S follows from that of Y. An important observation is that a map S of k branches stands for the fact that the farthest landing point occurs in the k-th hump. That is, the first branch is the set of all points that get mapped to the k-th hump, the second branch consists of the points that get mapped to the $(k-1)$-st hump, etc.

In the case of a one branch map, S, it can be shown (see Boyarsky and Góra [9]) that S has an attracting fixed point as illustrated in Figure 3.7. In this analysis the circular segments of the base curve were approximated to parabolic, thus allowing for an explicit computation of the range map $S(s)$. An estimate for the number of branches was made depending on the speed, simply by finding the larger root of the approximated expression in (3.2) when the launch point is $s_0 = 0$. This computation leads to the maximum value of landing point, the integer value of

which corresponds to the number of branches of the map S. This value is $[\omega^2]$. Thus with this approximation it can be shown that the map $S(s)$ consists of one branch if $1 < \omega^2 < 2$. Furthermore, this approximation makes it possible for Góra and Boyarsky to establish analytically the existence and explicit form of an attracting fixed point $s_f = 1/2 - 1/2\omega^{-2}$ for $1 < \omega^2 < 2$. Thus, when the linear speed of the wheel is in this range the system eventually enters a periodic regime, in the sense that landing (i.e. drilling) occurs only at the fixed point s_f. It can further be shown that when $\omega^2 > 2$ there are no attracting fixed points and drilling is uniform. Numerical analysis in the exact case supports Góra's results, and suggests that only the range $\omega^2 > 2$ is of interest.

An important result on acims is the Lasota-Yorke Theorem [7], which states that if $S_q : [0, q] \to [0, q]$, where $q \in (0, 1)$, is a piecewise C^2 function with finitely many pieces, having the property $\inf_{x\in[0,q]} |S_q'(x)| > 2$, then an absolutely continuous invariant measure exists. In the drill map of n branches $S'(x) > 1$ for all x, except on interval I near $x = 1$. This motivates the idea of inducing a map on a subinterval $[0, q] \subset [0, 1]$. The new induced map $S_q : [0, q] \to [0, q]$ has the property $S'(x) > 1$ for all x. Thus, there exists a $p \in \mathbb{N}$ such that $S_q^p(x)$ is a map with finitely many branches which satisfies the condition $\inf_{x\in[0,q]} |(S^p)'(x)| > 2$. For this map we can conclude that an acim exists due to Lasota-Yorkes's result. In the next section the idea of induced transformations will be developed, and we will discuss how one can lift the Lasota-Yorke result to the original unit interval map S.

3.4 Induced Maps and Their Invariant Measures

In this section let S be an ergodic measure preserving transformation on a normalized measure space $(X, \mathcal{B}, \mu)$.

Definition 3.2 *A set A is called a* **recurrent subset** *of X if for all $x \in A$ there*

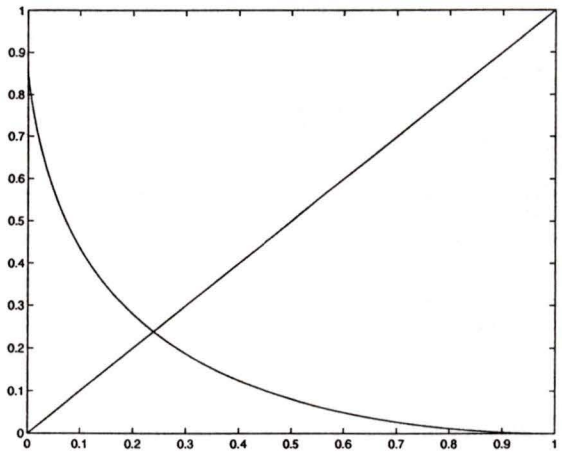

Figure 3.7: Depicted is the trajectory map for a midrange speed ($1 < \omega^2 < 2$) along with the line $y = x$ to illustrate the fixed point property of the map S. In this case, $\gamma = 9.55 \times 10^{-2}$ and $\omega = 1.37$.

exists an $n(x) \geq 1$, *such that* $S^{n(x)}(x) \in A$. *Define the* **first return time function** *by* $N(x) = \min\{n(x) | S^{n(x)} \in A\}$. *The* **first return time transformation** *or* **induced transformation** *on* A, *denoted by* $S_A(x)$, *is defined to be*

$$S_A(x) = S^{N(x)}(x) \tag{3.3}$$

for all $x \in A$.

REMARK: According to the Poincaré Recurrence Theorem (see [9]) for a measure preserving transformation S the right hand side of expression (3.3) is necessarily finite almost everywhere.

We illustrate the concept of induced transformations in the next example.

EXAMPLE 1: Let $S(x) = 2x(\text{mod } 1)$ and let $A = [0, 1/2]$. We construct the induced map S_A in Figure 3.8 by obtaining the first return time function $N(x)$.

On $A_1 = [0, 1/4]$, $N(x) = 1$. Namely $S(1/4) = 1/2$ and for $x \in A_1$, $S(x) \in [0, 1/2]$. Hence on A_1, $S_A(x) = S(x)$. Similarly on $A_2 = [2/8, 3/8]$, $N(x) = 2$, that

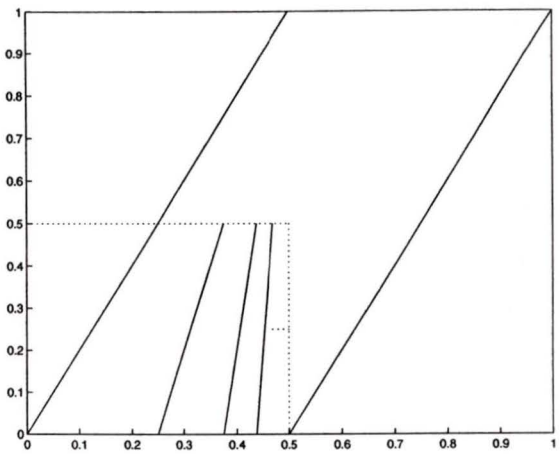

Figure 3.8: The induced transformation $S_{[0,1/2]}(x)$ corresponding to the dyadic map $S(x) = 2x(\text{mod } 1)$ on $[0, 1]$.

is $S^2(3/8) = 1/2$ and for $x \in A_2$, $S(x) \notin A$ and $S^2(x) \in A$. Continuing in this way we obtain $N(x) = k$ on $A_k = [s/2^{k+1}, (s+1)/2^{k+1}]$, where $s = \sum_{i=1}^{k-1} 2^i = 2^k - 2$. Hence $S_A(x) = S^k(x)$ for $x \in A_k$. The resulting map is illustrated in Figure 3.8.

Let (X, ν) be a measure space and $S : X \to X$ be a nonsingular transformation. Let $A \subset X$ be a recurrent subset and suppose S_A is the transformation obtained by inducing the map S on A. Our interest in induced mappings arises from Lasota and York's result from 1973 (see [7]). It states that if a transformation $S_A : [0, q] \to [0, q]$ has finitely many branches and is piecewise monotone and C^2 with the property $\inf_{x\in[0,q]} |S'_A(x)| > 2$, then an acim exists for S_A on $[0, q]$. The example above showed how an induced transformation may be constructed on a subset of the unit interval $A = \bigcup_{k=1}^{\infty} A_k$, where $A_i \cap A_j = \emptyset$ and the first return time function on A_k takes the value k. In this case however the induced map has infinitely many branches, thus Lasota-York's Theorem cannot be applied. We will see that the induced transformation on the rock drill map has finitely many branches, and deduce that an acim on the induced map S_A exists. The idea is to extend this result

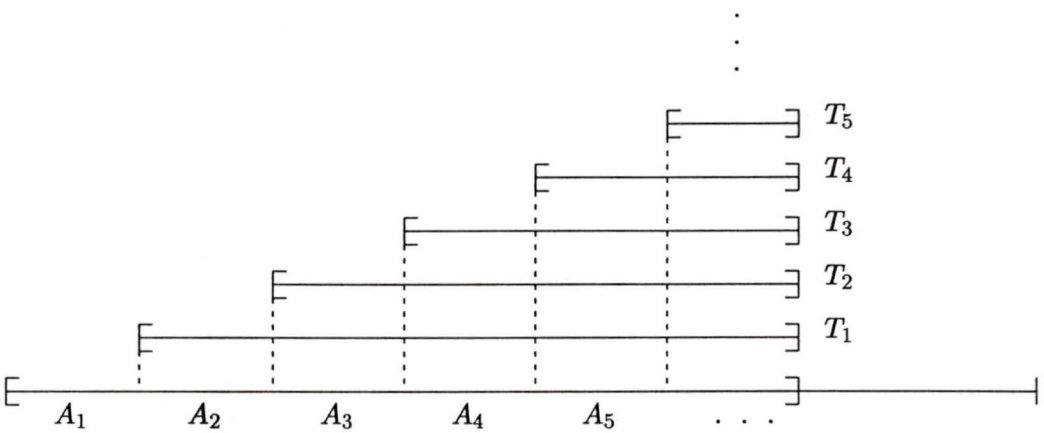

Figure 3.9: The sets A_k and T_k, for $k \in \mathbb{N}$. When $k = 0$, $T_0 = A$.

from S_A to the unit interval map S, i.e. the original rock-drill map. With this notation in mind we would like to relate the invariant density function of the induced transformation S_A to that of the original transformation S. Referring to figure 3.9 define $A_k = \{x \in A \,|\, N(x) = k\}$. Notice that since A is recurrent $A = \cup_{k=1}^{\infty} A_k$ disjointly. The next theorem extends the result of existence of an acim from the induced to the original map.

Theorem 3.3 *Let $S : [0,1] \to [0,1]$ be a measurable transformation and let A be a recurrent subinterval of $[0,1]$. Let $S_A : A \to A$ be the induced map, preserving the measure, μ_A. Let B be an element of the Borel $\sigma-$algebra on $[0,1]$ Then the lift of μ_A to the unit interval, denoted by μ, defined by*

$$\mu(B) = \sum_{k=1}^{\infty} \sum_{i=1}^{k} \mu_A \left(S^{-i+1} B \cap A_k \right) \tag{3.4}$$

is an invariant measure for the transformation S.

We prove this in a series of Lemmas.

Lemma 3.4 *Let B be a measurable set in X. Then*

$$S_A^{-1}(B \cap A) = \bigcup_{k=1}^{\infty} S^{-k}B \cap A_k$$

as a disjoint union.

Proof: The union above is disjoint since the A_k are disjoint. Now,

$$\begin{aligned}
x \in \bigcup_{k=1}^{\infty} S^{-k}B \cap A_k &\Leftrightarrow \exists k, \text{ such that } x \in A_k \text{ and } x \in S^{-k}B \\
&\Leftrightarrow \exists k, \text{ such that } x \in A_k \text{ and } S^k(x) \in B \\
&\Leftrightarrow \exists k, \text{ such that } x \in A_k \text{ and } S_A(x) \in B \\
&\Leftrightarrow \exists k, \text{ such that } x \in A_k \text{ and } S_A(x) \in B \cap A \\
&\Leftrightarrow x \in A \text{ and } S_A(x) \in B \cap A \\
&\Leftrightarrow x \in A \cap S_A^{-1}(B \cap A) \\
&\Leftrightarrow x \in S_A^{-1}(B \cap A) \quad \square
\end{aligned}$$

Lemma 3.5 *The measure μ defined by expression 3.4 is invariant under the transformation S.*

Proof: We show that $\mu(S^{-1}B) = \mu(B)$.

$$\begin{aligned}
\mu(S^{-1}B) &= \sum_{k=1}^{\infty}\sum_{i=1}^{k} \mu_A(S^{-i}B \cap A_k) \\
&= \mu(B) + \sum_{k=1}^{\infty} \mu_A(S^{-k}B \cap A_k) - \sum_{k=1}^{\infty} \mu_A(B \cap A_k) \\
&= \mu(B) + \mu_A(S_A^{-1}(B \cap A)) - \sum_{k=1}^{\infty} \mu_A(B \cap A_k) \qquad \text{by Lemma 3.4} \\
&= \mu(B). \quad \square
\end{aligned}$$

Lemma 3.6 *Suppose S is nonsingular w.r.t. the measure ν and $\mu_A \ll \nu|_A$ with $\frac{d\mu_A}{d\nu|_A} = g_A$. Let the operator $\mathcal{L} : L^1 \to L^1$ be the Perron-Frobenius operator for*

$S : X \to X$, Then the measure μ defined by

$$\frac{d\mu}{d\nu} = \sum_{k=1}^{\infty} \sum_{i=1}^{k} \mathcal{L}^{i-1}(\chi_{A_k} g_A) \tag{3.5}$$

is absolutely continuous w.r.t ν and agrees with the lift of μ_A defined in expression (3.4).

Proof: With μ defined by Equation 3.5, it can easily be shown that $\mu \ll \nu$. We need only verify the definition of μ. Let $B \subset X$ be a measurable set. Then

$$\begin{aligned}
\mu(B) &= \sum_{k=1}^{\infty} \sum_{i=1}^{k} \int_{S^{-i+1}B \cap A_k} g_A \, d\nu \\
&= \sum_{k=1}^{\infty} \sum_{i=1}^{k} \int_{S^{-i+1}B} \chi_{A_k} g_A \, d\nu \\
&= \sum_{k=1}^{\infty} \sum_{i=1}^{k} \int_{B} \mathcal{L}^{i-1}(\chi_{A_k} g_A) \, d\nu \qquad \text{by definition of } \mathcal{L}.
\end{aligned}$$

We apply the Monotone Convergence Theorem to the increasing sequence of non-negative functions $f_j = \sum_{k=1}^{j} \sum_{i=1}^{k} \mathcal{L}^{i-1}(\chi_{A_k} g_A)$ for $j = 1, 2 \ldots$, converging to $f = \sum_{k=1}^{\infty} \sum_{i=1}^{k} \mathcal{L}^{i-1}(\chi_{A_k} g_A)$. Thus we obtain

$$\mu(B) = \int_B \left[\sum_{k=1}^{\infty} \sum_{i=1}^{k} \mathcal{L}^{i-1}(\chi_{A_k} g_A) \right] d\nu. \quad \square \tag{3.6}$$

Equation 3.6 leads to a natural definition for the invariant density function of the measure μ. Define

$$g = \sum_{k=1}^{\infty} \sum_{i=1}^{k} \mathcal{L}^{i-1}(\chi_{A_k} g_A). \tag{3.7}$$

The above calculation shows that $g \in L^1$ and $||g|| = 1$. Furthermore, the sum in the definition converges in L^1. The next Lemma shows that g is a fixed point of the operator $\mathcal{L}$.

Lemma 3.7 *If g and $\mathcal{L}$ are as defined above, then $\mathcal{L}g = g$ a.e..*

We present two proofs.

Proof 1: By Lemma 3.5 and expression (3.5), $\mu \circ S^{-1} = \mu$ and $\mu = g\,d\nu$. Thus for all $B \subset X$ we have

$$\int_B \mathcal{L}g\,d\nu = \int_B g\,d\nu.$$

Hence $\mathcal{L}g = g$ a.e.. □

Proof 2: (Direct) Let $f \in L^1(A, \nu|_A)$ and $\mathcal{P} : L^1 \to L^1$ be the Perron-Frobenius operator for S_A. Then for all $x \in A$ Then

$$\begin{aligned}
\mathcal{P}f(x) &= \sum_{y \in A,\, S_A(y)=x} \frac{f(y)}{|S_A'|(y)} \\
&= \sum_{k=1}^{\infty} \left(\sum_{y \in A_k,\, S^k(y)=x} \frac{f(y)}{|(S^k)'|(y)} \right) \\
&= \sum_{k=1}^{\infty} \mathcal{L}^k(\chi_{A_k} f)(x).
\end{aligned}$$

Thus

$$\mathcal{P}f(x) = \sum_{k=1}^{\infty} \mathcal{L}^k(\chi_{A_k} f)(x). \tag{3.8}$$

Now,

$$\begin{aligned}
\mathcal{L}g &= \sum_{k=1}^{\infty} \sum_{i=1}^{k} \mathcal{L}^i(\chi_{A_k} g_A) \\
&= g + \sum_{k=1}^{\infty} \mathcal{L}^k(\chi_{A_k} g_A) - \sum_{k=1}^{\infty} \chi_{A_k} g_A \quad \text{by definition of } g \\
&= g + \mathcal{P}g_A - g_A \quad \text{by equation 3.8 and convergence in } L^1 \text{ of the infinite sum} \\
&= g. \quad \square
\end{aligned}$$

This proves Theorem 3.3 and defines and acim μ on S lifted from that of the induced map S_A.

REMARK: To make sense of Figure 3.9, define $T_j = \{x \mid \exists y \in A \text{ with } S^j(y) = x\}$ for $j = 0, 1 \ldots$. Note that while $A_i \cap A_j = \emptyset$ for $i \neq j$, T_i and T_j are not necessarily

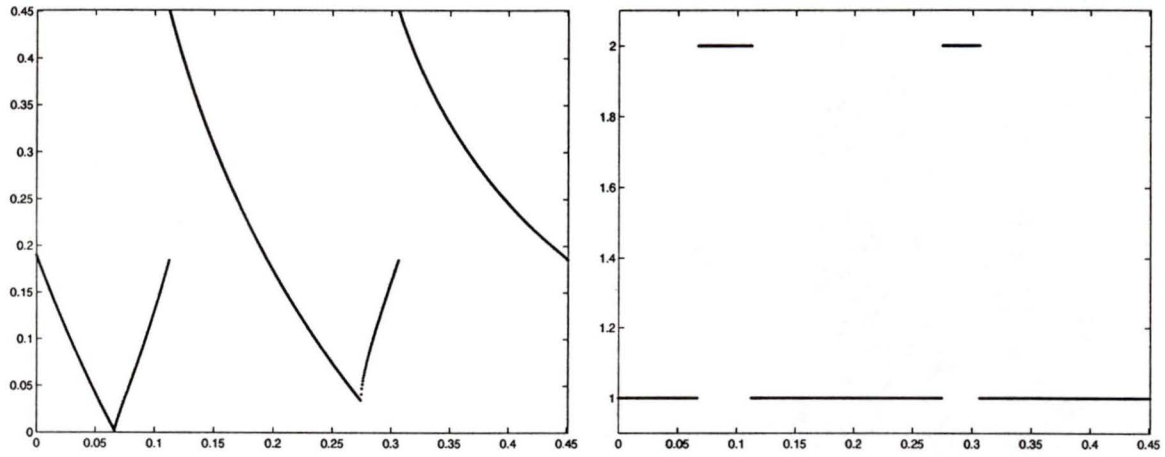

Figure 3.10: Left: Induced map $S_A : [0, 0.451] \to [0, 0.451]$ on the rock drill map S (based on usual parameters). Right: First return time function of the rock drill map defined by (3.3).

disjoint. To see this, refer to the dyadic map example. We induced the map $S(x) = 2x(\text{mod } 1)$ on $A = [0, 1/2]$. Then $T_1 \cap A_1 = [1/2, 3/4]$ and $T_2 \cap A_2 = [1/2, 3/4]$. Thus $T_1 \cap T_2 \neq \emptyset$.

The argument above shows that we may lift the measure of the induced map in order to obtain a measure for the original unit interval map, while preserving its invariance and absolute continuity. This allows us to use the Lasota-York result on existence of an acim to the oil drill map. In particular we may obtain the induced map $S_A : [0, q] \to [0, q]$, where q is such that $\inf_{x \in [0,q]} S'(x) > 1$. For a typical drill ($\gamma = 9.55 \times 10^{-2}$, $\omega = 1.78$) $q = 0.451$. Figure 3.10 shows the induced map S_A on $[0, 0.451]$. For a finite iterate of this map the hypothesis of Lasota-York's existence theorem holds. Hence an acim for the oil drill map exists. Thus the Birkhoff Ergodic method applies, provided the map is ergodic and we use the method outlined in Chapter 2 to compute the invariant density function of the oil drill map.

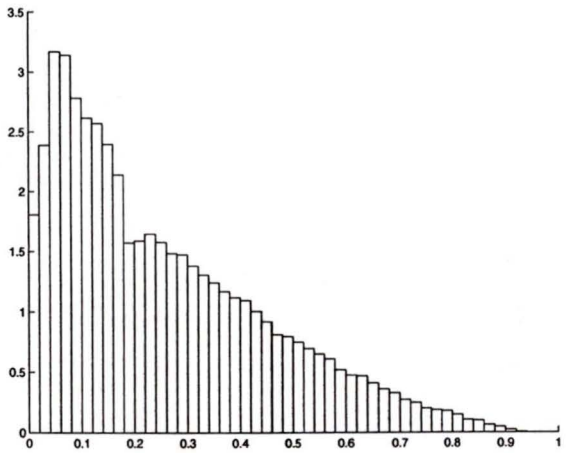

Figure 3.11: Shown here is the invariant density for the rock drill map with $\gamma = 9.55 \times 10^{-2}$, $\omega = 1.78$. In this particular example the orbit has a length of $n = 20,000$ iterations and a starting point of $\sqrt{2}/2$.

3.5 Birkhoff Theorem on the Rock Drill Model

Here we apply the Birkhoff Ergodic theory developed in Chapter 2 to the unit interval map S which models the dynamics of a rock drill. In the same fashion as in the examples in Chapter 2 we may obtain an invariant density by following the orbit of a given initial point. Let η be the partition of the unit interval of 50 equal sized bins. Using initial point $x = \sqrt{2}/2$ we may compute the Birkhoff ergodic averages of hits on each interval $E \in \eta$ and hence find an estimate for the invariant measure

$$\nu(E) \approx \frac{1}{n} \sum_{i=0}^{n-1} \chi_E \circ S^i(x) = \frac{\#\{i < n : S^i(x) \in E\}}{n}.$$

Figure 3.11 shows the result for an orbit of length $n = 20,000$.

Figures 3.12 and 3.13 are the density function estimates on a 50 bin partition when the initial point is $x = \sqrt{2}/4$ and $x = \sqrt{3}/3$. These numerical estimates reveal a reasonable stability of the long orbit computations with respect to choice of initial point. Clearly the coarse structure of the approximate density function is being

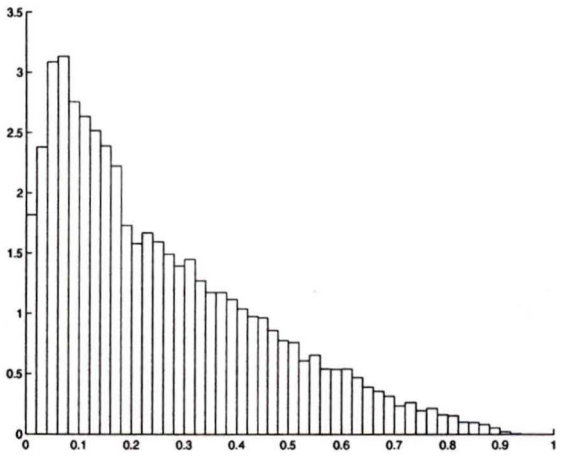

Figure 3.12: Shown here is the invariant density for the rock drill map on 50 bins with $\gamma = 9.55 \times 10^{-2}$, $\omega = 1.78$. In this estimate the orbit has a length of $n = 20,000$ iterations and a starting point of $\sqrt{2}/4$.

preserved between runs. This is in contrast to our experiments in Chapter 2 with the dyadic map. Nevertheless, one sees discrepancies between these runs, especially near the points where the density appears to be discountinuous. Figure 3.14 shows the invariant density function on 200 bins for the same initial point used for Figure 3.12. Since every point in the orbit is computed only within a certain accuracy, the longer the orbit, the more compounded the error. Thus refining the partition may not produce a more accurate estimate. This is one of the major drawbacks of this method. This motivates the use of an alternative method outlined in the next chapter.

3.6 Conclusion

The method used here to determine an estimate for the invariant density function was used in the earlier work of Lasota and Rusek [8]. As concluded in Chapter 2, there are several disadvantages to this method. Among them, this estimate of

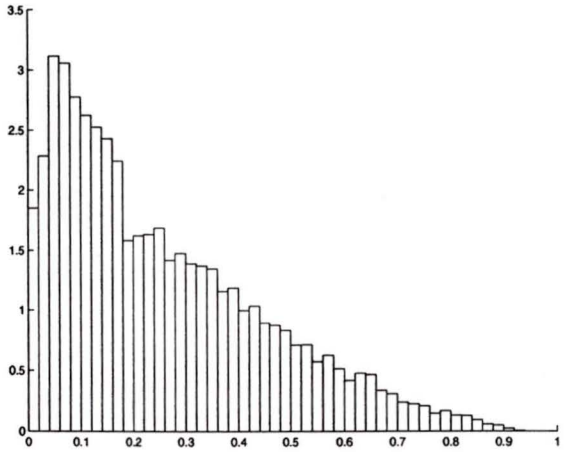

Figure 3.13: Shown here is the invariant density for the rock drill map with $\gamma = 9.55 \times 10^{-2}$, $\omega = 1.78$. Here the orbit has a length of $n = 20,000$ iterations and the starting point is $x_0 = \sqrt{3}/3$.

the invariant density function relies on the fact that the rock drill map is ergodic, which, due to its nature, is impossible to prove. Furthermore, due to the nature of the numerical derivation of the drill map, in obtaining the long orbits computer error is compounded, making the estimate uncertain. This and the relatively slow rate of convergence motivates the need of a different method for an estimate of the invariant density function, which will be discussed in the next chapter.

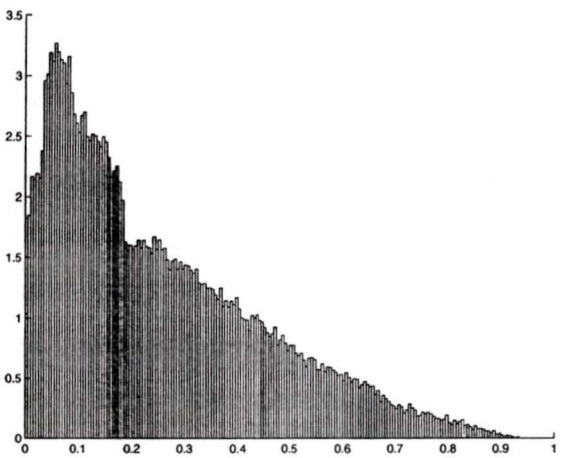

Figure 3.14: The invariant density for the rock drill map with $\gamma = 9.55 \times 10^{-2}$, $\omega = 1.78$. In this 200-bin estimate the orbit has a length of $n = 80,000$ iterations and a starting point of $\sqrt{2}/4$.

Chapter 4

Ulam's Method

4.1 Introduction

In this chapter we analyse an approximation scheme for invariant density estimates which was originally proposed by Ulam [5], known as Ulam's method. Here the Perron-Frobenius operator and its fixed point play an integral part. The convergence of Ulam's method depends on the form of the transition matrix associated with the transformation of interest. In Section 4.2 we will describe how this matrix can be obtained. The condition of convergence to an invariant density has been established for various classes of transformations. The Perron-Frobenius Theorem will be stated, providing the result we need to ensure the convergence of Ulam's method for the class of transformations with irreducible transition matrices.

4.2 Ulam's Method

In the subsequent material let $X \subset \mathbb{R}^n$ for some positive integer n be a compact metric space equipped with the Borel σ-algebra $\mathcal{B}(X)$. Let μ be a Borel measure on X.

Recall that $\nu(x) = \int f(x)\mu(dx)$ defines an absolutely continuous invariant measure with density f. As in the Birkhoff ergodic method for predicting the dynamics

and asymptotics of a transformation S, Ulam's method produces an estimate for the invariant density. However, rather than computing a long orbit for an arbitrarily chosen initial point x, Ulam's method uses the fixed point of an approximation to the Perron-Frobenius operator $\mathcal{L}$.

In Chapter 2 we defined the Perron-Frobenius operator $\mathcal{L}$ so that any fixed point of $\mathcal{L}$, $f_* \geq 0$ is the density of an invariant measure under S (Definition 2.9). We applied the Perron-Frobenius operator to the dyadic map (Example 4) in an iterative manner and observed the quick convergence to the invariant density function $f_* \equiv 1$ (see Figure 2.2). This asymptotic behaviour is in fact the feature carried into Ulam's method in obtaining an approximation of the true density corresponding to a given transformation. The details of this process are described in this section. Firstly we develop the notion of histogram measures beginning with the definition of a partition of X. Definition 4.1 is a generalization of Definition 2.19.

Definition 4.1 *Let (X, μ) be a measure space. Let $\eta = \{B_1, B_2, \ldots, B_n\}$, where $\mu(B_i) > 0$ for all i, $1 \leq i \leq n$. Then η is a* **partition** *of X of size n if $\cup_{i=1}^{n} B_i = X$ and $B_i \cap B_j = \emptyset$ for all i, j, $1 \leq i, j \leq n$. If in addition $\mu(B_i) = \mu(B_j)$ for all i, j, then we say that η is a* **uniform partition.**

Definition 4.2 *An absolutely continuous probability measure ν on X will be called a* **histogram measure** *over η if one may choose its density f to be constant on each $B_i \in \eta$. That is*

$$f = \sum_{B_i \in \eta} f_{B_i} \chi_{B_i} \quad \text{where } f_{B_i} \in \mathbb{R}^+$$

and

$$\|f\| = \sum_{B_i \in \eta} f_{B_i}\, \mu(B_i) = \nu(X) = 1.$$

The collection of such densities will be denoted by

$$\mathcal{D}_\eta = \Big\{ f \in L^1(X) \colon f = \sum_{B_i \in \eta} f_{B_i} \chi_{B_i},\ f_{B_i} \in \mathbb{R}^+,\ \forall B_i \in \eta,\ \|f\| = 1 \Big\}.$$

Notice that there is a one-to-one correspondence between the elements of $\mathcal{D}_\eta$ and the set of vectors $\{(\nu(B_1), \nu(B_2), \ldots, \nu(B_n)) \in (\mathbb{R}^+)^n : \sum_{i=1}^n \nu(B_i) = 1\}$. Throughout this thesis the representation of a histogram as an element in $\mathcal{D}_\eta$ and a vector in $(\mathbb{R}^+)^n$ will be used interchangeably. Depending on the representation χ_{B_i} can take two forms. Namely

$$\chi_{B_i} = \begin{cases} 0 & : \quad x \notin B_i \\ 1 & : \quad x \in B_i \end{cases}$$

when viewed as an element of $\mathcal{D}_\eta$, and

$$\chi_{B_i} = (0, \ldots, 1, \ldots, 0)$$

otherwise. From this point forward which form is used will be self evident from the context of where it is applied.

Given an absolutely continuous measure $\nu = f\, d\mu$, we can define the corresponding histogram measure ν_η by

$$\nu_\eta(A) = \sum_{B \in \eta} \frac{\mu(B \cap A)}{\mu(B)} \nu(B)$$

for every $A \in \mathcal{B}(X)$. We will show this is a histogram measure. First we define the **projection operator** of L^1 onto $\mathcal{D}_\eta$, which will allow for a natural derivation of the density function of the measure ν_η.

Definition 4.3 *Let $f \geq 0$ in L^1. Define the* **projection operator** *onto $\mathcal{D}_\eta$ by*

$$\Pi_\eta f = \sum_{B \in \eta} \left[\frac{1}{m(B)} \int_B f\, dm \right] \chi_B.$$

That is, given any $f \in L^1$, $\Pi_\eta f \in \mathcal{D}_\eta$, and if ν is an absolutely continuous measure with density f, then the measure ν_η has density $\Pi_\eta f$. Hence we will refer to Π_η as the **projection** of f into $\mathcal{D}_\eta(X)$.

To see the ν_η is in fact a histogram measure, consider $A \in \mathcal{B}(X)$. Then

$$\begin{aligned} \nu_\eta(A) &= \sum_{B\in\eta} \mu(B \cap A)\frac{1}{\mu(B)} \int_B f \, d\mu \\ &= \sum_{B\in\eta} \mu(A \cap B)\Pi_\eta f|_B \\ &= \int_A \sum_{B\in\eta} \chi_B \Pi_\eta f \, d\mu. \end{aligned}$$

Therefore ν_η is a histogram measure with density $\Pi_\eta f$.

The following describes an approximation scheme proposed by Ulam as a way of obtaining an approximate invariant density for S, embedded in $\mathcal{D}_\eta(X)$, using the fixed point of the Perron-Frobenius operator.

Definition 4.4 *Let $\mathcal{L}$ be the Perron-Frobenius operator for the nonsingular transformation S and $\eta = \{B_1, B_2, \ldots, B_n\}$ be a partition of X. Then the operator $\mathcal{P}_\eta : \mathcal{D}_\eta \to \mathcal{D}_\eta$ is called the* **Ulam approximation** *of $\mathcal{L}$ corresponding to S and is defined by*

$$\mathcal{P}_\eta = \Pi_\eta \circ \mathcal{L}.$$

A normalized fixed point of $\mathcal{P}_\eta$ is an **Ulam approximate density**.

To make sense of the this definition suppose μ is Lebesgue measure and let $\mu(X) = 1$. Define the row stochastic matrix $P_\eta = (p_{ij})$ by

$$p_{ij} = \frac{\mu(B_i \cap S^{-1}B_j)}{\mu(B_i)} \tag{4.1}$$

so that p_{ij} is the transition probability from the state B_i to the state B_j. In fact, if we let $P_\eta^k = (p_{ij}^{(k)})$ it can be verified by simply using matrix multiplication that $p_{ij}^{(k)}$

is the probability of ending up in state B_j after k iterations given that you start in state B_i. Notice that $\mathcal{P}_\eta$ is an operator on $\mathcal{D}_\eta$, whereas P_η is a matrix of transition probabilities. We will show that P_η is in fact a matrix representation of the operator $\mathcal{P}_\eta$. Define a basis for $\mathcal{D}_\eta$, $\{d_i\}_{i=1}^n$, by

$$d_i = \frac{1}{\mu(B_i)}\chi_{B_i} \text{ for } i = 1, 2, \ldots, n \tag{4.2}$$

and consider the standard basis for $\mathbb{R}^n$, $\{\vec{e_j}\}_{j=1}^n$, defined by $(\vec{e_j})_i = 1$ if $i = j$, and $(\vec{e_j})_i = 0$ otherwise. Applying Definitions 2.1 and 4.3,

$$\begin{aligned}
\mathcal{P}_\eta d_i = \Pi_\eta \circ \mathcal{L}(d_i) &= \sum_{B_j \in \eta} \frac{1}{\mu(B_j)} \int_{B_j} \mathcal{L} d_i dx \, \chi_{B_j} \\
&= \sum_{B_j \in \eta} \left(\int_{S^{-1}B_j} d_i \, dx \right) d_j \\
&= \sum_{B_j \in \eta} \left(\int_{S^{-1}B_j} \frac{\chi_{B_i}}{\mu(B_i)} \, dx \right) d_j \\
&= \sum_{B_j \in \eta} \frac{\mu(B_i \cap S^{-1}B_j)}{\mu(B_i)} \, d_j \\
&= \sum_{B_j \in \eta} a_j d_j
\end{aligned}$$

Thus the vector $\vec{a}$ satisfies $\vec{a} = \vec{e_i} P_\eta = i^{\text{th}}$ row of P_η, and since $(\vec{a})_j = (\vec{e_i} P_\eta)_j = p_{ij}$, we see that the matrix representation of $\mathcal{P}_\eta$ is given by $P_\eta = (p_{ij})$ where p_{ij} are as defined in (4.1).

One can verify that matrix P_η has nonnegative entries and it is row stochastic. This follows from the fact that $\mu(\cdot)$ is a probability measure (i.e. $\mu(X) = 1$) and η is a partition of X. This enables us to obtain an Ulam approximate density, $\vec{u} = (u_1, u_2, \ldots, u_n)$ by computing the invariant vector of matrix P_η, provided it exists. This vector will be the invariant density vector w.r.t. basis $\{\vec{d_j}\}_{j=1}^n$. Subsequently,

we may find the standard basis representation of the density vector, using

$$f = \sum_{B_j} u_j d_j, \tag{4.3}$$

where d_j, $j = 1, \ldots, n$ are as defined in 4.2. The Perron-Frobenius theorem provides sufficient conditions for the existence of a fixed vector for matrix P_η.

Theorem 4.5 *(Perron-Frobenius Theorem) Let $A \neq 0$ be an irreducible[1] stochastic matrix. Then A has a strictly positive eigenvector[2] $\mathbf{x}_0$ with corresponding eigenvalue $\lambda = 1$ that is geometrically simple[3]. Furthermore if β is another eigenvalue of A, then $|\beta| \leq 1$, and any strictly positive eigenvector of A is a positive multiple of $\mathbf{x}_0$.*

Proof. See Seneta [1]. □

Therefore $\mathcal{P}_\eta$ has a dominant eigenvalue $\lambda = 1$, to which there corresponds a right and left positive eigenvector, in particular (apply Theorem 4.5 to P_η and P_η^T)

$$P_\eta \mathbf{1} = \mathbf{1} \quad \text{and} \quad \exists \text{ unique } \mathbf{x}_0 \text{ s.t. } \mathbf{x}_0 P_\eta = \mathbf{x}_0 \text{ and } \sum_j (\mathbf{x}_0)_j = 1.$$

Hence $\mathbf{x}_0$ is an Ulam approximate density function from Definition 4.4. To obtain this vector we note that it is an eigenvector of P_η. The following theorem provides an alternate method, which in some cases is a more efficient way for obtaining this eigenvector.

Theorem 4.6 *Suppose $P = (p_{ij})$ is a nonnegative stochastic irreducible matrix, and let $P^k = (p_{ij}^{(k)})$. If $\mathbf{x}_0 = (x_1, x_2, \ldots, x_n)$ is the normalized left Perron-Frobenius eigenvector then*

$$\lim_{k \to \infty} p_{ij}^{(k)} = x_j \quad \text{for } j = 1, 2, \ldots, n.$$

---

[1] A matrix A is irreducible if for all (i, j) $\exists n$ such that $(A^n)_{ij} > 0$.

[2] A vector is considered positive if all its entries are positive.

[3] An eigenvalue is geometrically simple if its corresponding eigenspace is one-dimensional.

Proof. See Feller [3]. □

So Theorem 4.5 provides us with a unique invariant density vector and Theorem 4.6 estimates it within arbitrarily small error. In fact, the normalized positive eigenvector $\mathbf{x}_0 = (x_1, x_2, \ldots, x_n)$ corresponding to eigenvalue $\lambda = 1$ satisfies the condition

$$\min_i p_{ij}^{(k)} \leq x_j \leq \max_i p_{ij}^{(k)}$$

for all j, $1 \leq j \leq n$, where $P^k = (p_{ij}^{(k)})$. Indeed, from $\mathbf{x}_0 P = \mathbf{x}_0$ we have $\mathbf{x}_0 P^k = \mathbf{x}_0$, thus for each j,

$$\begin{aligned} \sum_{i=1}^{n} p_{ij}^{(k)} x_i &= x_j \\ \Rightarrow \sum_{i=1}^{n} \min_i p_{ij}^{(k)} x_i &\leq x_j \\ \Rightarrow \min_i p_{ij}^{(k)} \sum_{i=1}^{n} x_i &\leq x_j \end{aligned}$$

Since $\sum_{i=1}^{n} x_i = 1$, we have $\min_i p_{ij}^{(k)} \leq x_j$, and with a similar argument we obtain $x_j \leq \max_i p_{ij}^{(k)}$.

In order to be able to apply Theorems 4.5 and 4.6 P_η must be irreducible. That is, it is necessary that for each (i, j) after n steps (i.e. n iterations of the map S for some $n \in \mathbb{N}$), bin B_i meets bin B_j with positive probability.

The convergence in Ulam's method is directly related to that in Theorem 4.6, the rate of which will be observed numerically in the subsequent chapter. We will see that this method provides fast convergence to the invariant density of the rock drill map. The following theorem is of particular importance in applications, as it gives sufficient conditions for convergence in Ulam's method.

Theorem 4.7 *Let $S : [0,1] \to [0,1]$ be a piecewise C^2 function with $\inf_{x \in [0,1]} |S'| > 2$. Suppose $\mathcal{L}$ is the Perron-Frobenius operator of S and η a unifiorm partition of*

$[0,1]$ *of size* n. *If* $\mathcal{L}$ *has a unique fixed point, then for any positive integer* n, P_η *has a fixed point* f_n *in* $\mathcal{D}_\eta$ *with* $||f_n|| = 1$. *Furthermore, as* $n \to \infty$ *the sequence* $\{f_n\}$ *converges in* L^1 *norm to the fixed point of* $\mathcal{L}$.

Proof: See [4].

For the oil drill map the only hypothesis of Theorem 4.7 we know analytically is the existence of a fixed point of the Perron-Frobenius operator . The argument involves inducing the unit interval map, applying Lasota-Yorke's existence Theorem [7] on the induced map, and lifting the existence result to the unit interval map using the discussion in Section 3.4. One could apply Ulam's method on the induced map (which does satisfy the hypothesis of Theorem 4.7). However, in this thesis Ulam's method will be applied to the full transformation instead. Numerical evidence of the validity of this idea is provided in the next chapter.

The next example is an illustration of Ulam's method, as well as a contrast with the Birkhoff ergodic method discussed in Chapter 2.

EXAMPLE: Consider the dyadic map and refer to Figure 2.1. Suppose η is the four-bin partition of equal subintervals B_i. For each pair of bins B_i, B_j compute the corresponding ratio in (4.1) and form the matrix $P_\eta = (p_{ij})$. The resulted matrix is

$$P_\eta = \begin{pmatrix} \frac{1}{2} & \frac{1}{2} & 0 & 0 \\ 0 & 0 & \frac{1}{2} & \frac{1}{2} \\ \frac{1}{2} & \frac{1}{2} & 0 & 0 \\ 0 & 0 & \frac{1}{2} & \frac{1}{2} \end{pmatrix}.$$

Simple computation shows that $P^2 > 0$, hence the matrix P is irreducible, and by Theorem 4.5 it has a unique positive eigenvector, in particular the left Perron eigenvector,

$$\mathbf{x}_0 = \begin{pmatrix} \frac{1}{4} \\ \frac{1}{4} \\ \frac{1}{4} \\ \frac{1}{4} \end{pmatrix}.$$

For this low dimension example it is easy to compute x_0 directly from the definition of eigenvector. For more refined partitions it may be required to use Theorem 4.6 to find x_0. Observe that for the dyadic map high powers of the matrix P quickly converge to the matrix of columns $\mathbf{x}_0$. Indeed

$$P_\eta^n = \frac{1}{4}\begin{pmatrix} 1 & 1 & 1 & 1 \\ 1 & 1 & 1 & 1 \\ 1 & 1 & 1 & 1 \\ 1 & 1 & 1 & 1 \end{pmatrix}$$

for $n \geq 2$. Thus the invariant density function is given by

$$f = \sum_{B_i \in \eta} a_i d_i = \sum_{j=1}^{4} \frac{1}{4} \frac{1}{(1/4)} \chi_{B_j} \equiv 1,$$

as expected (Theorem 2.17). Recall from Chapter 2 that using Birkhoff method for computing the invariant density function a δ-function was obtained. As we pointed out earlier this is due to the fact that in the computer language the floating point representation of every real number is a dyadic rational, and all such points eventually get mapped to the fixed point $x = 0$. That is, all values of the initial launch point x_0 fall within the exceptional set of Birkhoff's Theorem, yielding a δ-function peaked at 0. Ulam's method bypasses this problem and produces the true invariant density, proving to be the more robust method between the two.

4.3 Conclusion

Relatively easy to implement on a computer (see Appendix A), Ulam's method offers an alternative to the Birkhoff method of numerical approximation of invariant measures. In Ulam's method rather than computing long orbits we are concerned with computing the eigenvector of the transition matrix associated with the map of interest. This significantly simplifies the numerics and offers a more efficient way to estimate the invariant density function. Furthermore, contrary to the Birkhoff

method, Ulam's method does not depend on the choice of initial point, therefore addressing the issue of the exceptional set of points in Birkhoff's Theorem. The rate of convergence of Ulam's method will be observed numerically in Chapter 5 for the specific example of the drill map.

Chapter 5

Ulam's Method Applied

5.1 Introduction

The objective in this chapter is to obtain Ulam's approximate density for the oil drill map using the method outlined in the previous chapter. An estimate for this invariant density function was computed using the Birkhoff method in Chapter 3. We discussed that the Ulam's method is likely to be more reliable. We will see that in this case the computed density is consistent with the course structure obtained in Chapter 3, but more stable with respect to fine detail. The run time in both methods is comparable as can be seen in Appendix A. This is because in the Birkhoff method an orbit of length n is computed by evaluating n iterations of the drill map. In Ulam's method we estimate the drill map for n equally spaced values in the domain. The main advantage of Ulam's method, as mentioned earlier in this thesis, is in the nature of these evaluations. In contrast with the Birkhoff method, here the error is not compounded over the course of the evaluations. Thus, in Section 5.2 our goal is to produce the invariant density function for a given value of the speed, and subsequently convince the reader of the accuracy of this estimate with numerical evidence.

In Section 5.3 we will compute the average amount of energy that is transferred

into the rock by the drill in one revolution of the wheel. This will be done numerically using the Birkhoff Ergodic Theorem along with the invariant density estimate produced by Ulam's method.

5.2 Density Estimate Using Ulam's Method

Consider the oil drill map S discussed in Chapter 3. Suppose η is a partition of the unit interval of 50 equal sized bins. To apply Ulam's method to the map S for each pair of bins B_i, B_j we need to compute the ratio defined by (4.1), and hence obtain $P_\eta = (p_{ij})$. Recall from Section 3.2 that there is no closed form expression for the map S available to us, so it was determined numerically rather than analytically. This means that we do not have a precise way to obtain the Lebesgue measure of a given set, $S^{-1}B_j$. Therefore a Monte-Carlo type estimate is used. That is

$$p_{ij} = \frac{\mu(B_i \cap S^{-1}B_j)}{\mu(B_i)} = \frac{\#\text{points in } B_i \cap S^{-1}B_j}{\text{total } \#\text{points in } B_i}. \tag{5.1}$$

In this manner we form the Ulam matrix P_η. To check irreducibility we need to see that for all i, j, $p_{ij}^{(k)} > 0$ for some positive integer k, namely that one can get from bin B_i to bin B_j in finitely many steps. This was studied by computing a high power of the matrix for several values of the size of the partition η. The power of the matrix was observed to have positive entries for each of those values, thus suggesting the condition of irreducibility. Therefore by Theorem 4.5 there is a unique positive eigenvector corresponding to the matrix P_η of the transformation S which serves as Ulam's approximate density function. The vector in question was computed and it produced an invariant density function shown in Figure 5.1. The algorithms are described in Appendix A. It should be noted that for each i, j expression (5.1) is evaluated using the points that define the drill map S. This is done by counting the number of times that $S(x) \in B_j$ over all $x \in B_i$. The density in Figure 5.1 corresponds to the rock drill map with usual parameters and a speed of

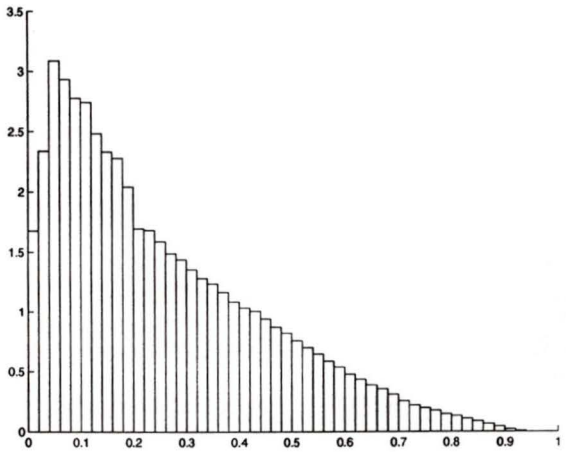

Figure 5.1: Shown here is the Ulam approximate density on a fifty bin partition for the oil drill map with $\gamma = 9.55 \times 10^{-2}$, $\omega = 1.78$. The drill map S and the matrix P_η in expression (5.1) were defined with 20,000 function evaluations.

$c = 1.0$ ms^{-1}. Notice the agreement with the course structure of the corresponding picture produced using the Birkhoff ergodic method (see Figure 3.11).

Refining the partition gives an even better estimate for the invariant density function. It should be noted that for an accurate refinement we need to maintain the number of points per bin the same, namely the ratio between number of function evaluations to define the drill map and the number of bins will be preserved from one estimate to the next. Figure 5.2 shows the density function obtained when a 100-bin partition is used. Further refinement shows the fast convergence of the estimated density function and the limiting behaviour on the dynamics of the oil drill map. Figures 5.3 and 5.4 give an estimates for the invariant density function over a 200 and a 300-bin partition respectively when the map is defined with 80,000 and 120,000 function evaluations for $c = 1.0$ ms^{-1}. Notice the discontinuities in the density estimates near $x = 0.02$, $x = 0.1$ and $x = 0.2$. Figure 5.5 shows the

difference-error function $e_{50}(x)$ for the 50 and 300-bin estimate, defined by

$$e_{50}(B_i) = f_{300} - f_{50}(B_i)$$

where $f_{50}(B_i)$, $i = 1, \ldots, 50$ is the i^{th} component of the Ulam invariant density vector on 50 bins, and $f_{300}(B_i)$, $i = 1, \ldots, 50$, was found by downsampling the 300-bin estimate, found by Ulam's method, into a 50-bin estimate. The analogous computation was done for the difference-error function e_{100} between the 300 and 100-bin estimates in Figure 5.6. Notice that in both cases the error function peaks around $x = 0.1$ and $x = 0.2$. For those bins, where the true invariant density function is discontinuous, the error function peaks up to a difference of 0.3 in absolute value, yet everywhere else the error remains small in comparison. When a certain bin, B_i, in the 50-bin estimate falls over a discontinuity, the discretisation process fails to detect it, and it produces an average over neighbouring behaviour, contributing to high error. This clearly suggests that the true density function is indeed discontinuous. While the discretisation process is similar in the Birkhoff method, the error function is much more unstable, thus failing to provide clear evidence for discontinuities.

Figures 5.7, 5.8, 5.9 and 5.10 depict the 50, 100, 200 and 300-bin estimates for the invariant density function when the speed is $c = 1.4$ ms^{-1}. Figures 5.11 and 5.12 show the difference-error function computed using the 300 and 50-bin estimates, and the 300 and 100-bin estimate. In both figures the error function peaks around $x = 0.08$, $x = 0.12$ and $x = 0.22$, suggesting that the density function is discontinuous at those values of x. However, because the jumps in this case are not as dramatic as in the case when $c = 1.0$ ms^{-1}, the error function remains within an amplitude of 0.08 for e_{50} and 0.037 for e_{100}.

REMARK: To apply Ulam's method, the conditions of Theorem 4.7 must be satisfied. Namely, it is necessary that

1. The drill map S is piecewise C^2,

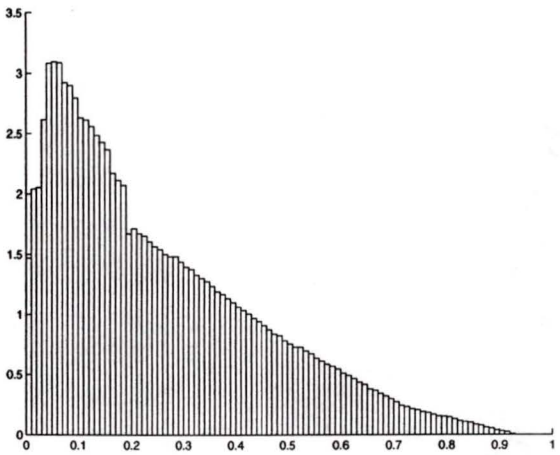

Figure 5.2: Shown here is the Ulam approximate density on a 100-bin partition for the oil drill map with $\gamma = 9.55 \times 10^{-2}$, $\omega = 1.78$. The drill map was defined with 40,000 function evaluations.

2. $\inf_{x\in[0,1]} S'(x) > 2$, and

3. The Perron-Frobenius operator P corresponding to S has a unique fixed point.

Condition 1 is satisfied based on the nature of the drill map. Conditions 2 and 3 are satisfied for the induced map corresponding to the drill map, making Ulam's method applicable to the induced map. It is possible to compute the invariant density distribution vector on the induced map, thereafter lift the result to the unit interval map, using formula (3.7). In this thesis, however, Ulam's method will be applied directly to the unit interval map. Numerically we will obtain evidence for the validity of this approach.

In Lasota-Rusek's [8] approach the invariant density function for a given value of ω^2 was approximated to γ-distributions based on 50-bin estimates produced by the Birkhoff method (where the orbits are taken of length 10,000 points). Lasota and Rusek obtained the best-fit γ-distribution, $\gamma(b,p)$, using the least squares method to find the parameters b and p, dependent on ω^2. They observed that as $\omega^2 \to \infty$

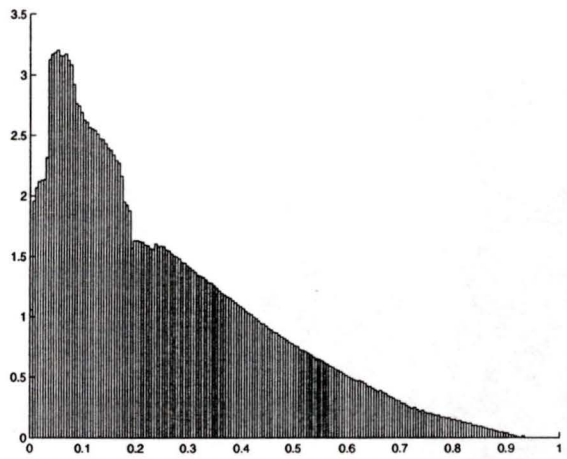

Figure 5.3: Shown here is the Ulam approximate density on a 200 bin partition for the oil drill map with $\gamma = 9.55 \times 10^{-2}$, $\omega = 1.78$. The drill map was defined with $80,000$ function evaluations.

the distribution function approaches a limiting γ distribution with set parameters, namely $\gamma_\infty = \gamma(9.68, 2.75)$. Lasota and Rusek used this limiting distribution to predict not only the efficiency, but also the asymptotics of the dynamics of the drill for high speeds. Note that the γ-distributions have continuous densities.

Our estimates suggest that the density for the rock drill map may not be continuous. Namely, at the end of each branch of the map S, due to the sudden change in weight in the Perron-Frobenius operator representation 2.3 (i.e. introducing the base of the new branch α with nontrivial derivative $S'(S_\alpha^{-1}x)$) the value of the Perron-Frobenius operator changes significantly. This gives rise to discontinuities in the resulting density. Especially indicative of this phenomena is the density in Figure 5.3 and its corresponding map in Figure 3.6. Observe that when $x = 0.04$ there is a sharp increase in the density function, which corresponds to introducing the weight of the low end of branch two of the unit interval map (see Figure 3.6, Left). In some cases, however the branch cut-off points do not seem to be reflected in the density function. As an example consider $x = 0.7$, where branch three ends.

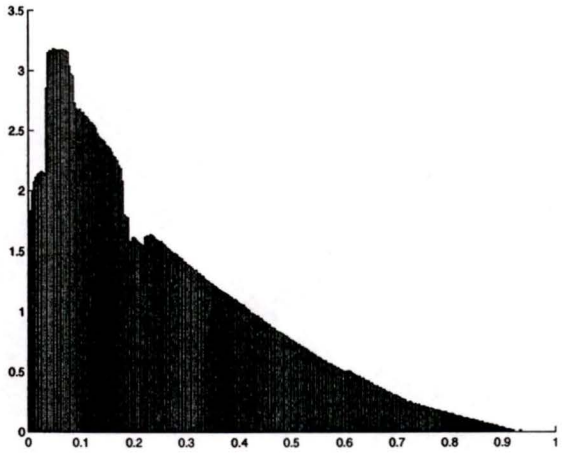

Figure 5.4: Ulam approximate density on a 300 bin partition for the oil drill map with $\gamma = 9.55 \times 10^{-2}$, $\omega = 1.78$. The drill map was defined with 120,000 function evaluations.

The top of this branch is fairly steep, making its weight at that end negligible. The density function appears continuous as a result.

5.3 Invariant Density Function Applied

In this section we will use the estimate for the invariant density function obtained in Section 5.2 to study the efficiency of the drill. For this we apply the Birkhoff Ergodic Theorem, namely given a function $f(s)$ we may compute the long-time average with initial point s_0 over the transformation S using the expression

$$\bar{f} = \lim_{n\to\infty} \sum_{k=1}^{n} f(S^k(s_0)) = \int_0^1 f(s)g(s)ds \tag{5.2}$$

where $g(s)$ is the invariant density function.

The efficiency of the drill will be studied using the average energy absorbed by the rock per revolution, denoted by h. Namely

$$h = K\,\bar{E}\,\frac{\pi d}{\Delta\bar{x}} \tag{5.3}$$

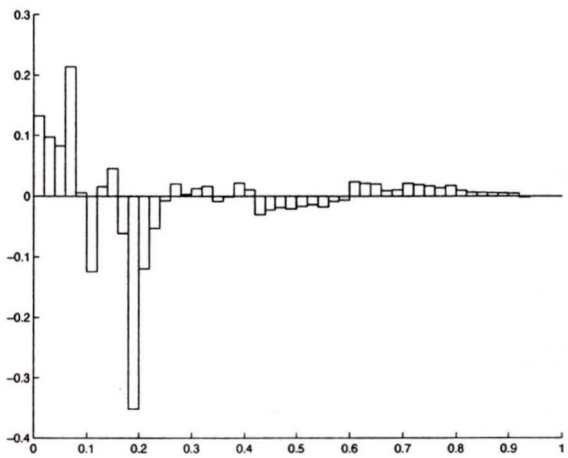

Figure 5.5: Shown here is the difference-error function between the 300-bin and 50-bin estimates in Figures 5.4 and 5.1.

where d is the diameter of the base of the drill bit, $\bar{E}$ is the average energy lost by the drill mechanism per hit, $\Delta\bar{x}$ is the average distance traveled by the wheel between two consecutive hits and $K < 1$ is a constant of efficiency, due to friction, heat transfer, etc. Thus,

$$h = K \times (\text{Avg Energy per Hit}) \times (\text{Avg Number of Hits per Revolution}).$$

We will compute $\bar{E}$ and $\Delta\bar{x}$ using expression (5.2).

As discussed in the earlier chapters, uniformity of drilling occurs only if $\omega^2 > 2$. In the case $0 < \omega^2 < 2$ drilling occurs only at the fixed point, an estimate for which was made by Góra [9]. This not only makes the work inefficient, but also increases the wear and tear of the drill. Thus in this case the ratio (5.3) does not reflect the efficiency of the drill and its computation will be omitted.

To find $\Delta\bar{x}$ when $\omega^2 > 2$ observe that $\Delta x = x_{n+1} - x_n = T(s_{n+1} - s_n) = TY(s)$, where $Y(s)$ is the range function computed in Chapter 3. Therefore

$$\Delta\bar{x} = T\int_0^1 Y(s)g_c(s)ds \tag{5.4}$$

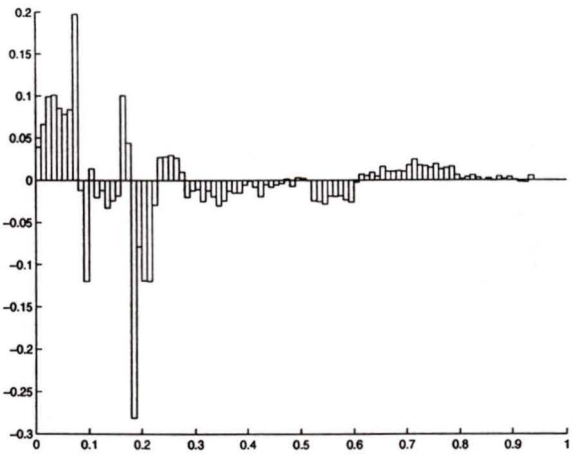

Figure 5.6: Shown here is the difference-error function between the 300-bin and 100-bin estimates computed over 120,000 and 40,000 function evaluations respectively when $\omega = 1.78$.

where $g_c(s)$ is the invariant density of the transformation S corresponding to linear speed c.

We now turn our attention to the calculation of the average energy per hit, lost by the drill, namely $\bar{E}$. Recall the mechanical assumptions of the drill/rock collisions described in Chapter 3. Suppose the previous collision took place at $x = x_{n-1}$, and the current collision at $x = x_n$ (in non-normalized variables - see Chapter 3 for notation). Let I be the moment of inertia about the mass centre and Ω_{pre} be the angular velocity just before collision. By König's Theorem (see [12]) the precollisional kinetic energy is

$$\frac{1}{2}M||\langle c, \frac{d\hat{w}}{dt}\rangle||^2 + \frac{1}{2}I\Omega_{\text{pre}}^2 = \frac{1}{2}M\left(c^2 + c^2\left(\frac{dw}{dx}\right)^2\right) + \frac{1}{2}I\Omega_{\text{pre}}^2$$

where $w = w(x, x_{n-1})$ is the vertical component of the trajectory leading from the $(n-1)$-st collision to the n-th. The derivative in this last expression is evaluated at $x = x_n$. At the moment of collision the vertical component of the wheel's mass centre trajectory is assumed to become zero with respect to the rock, therefore the

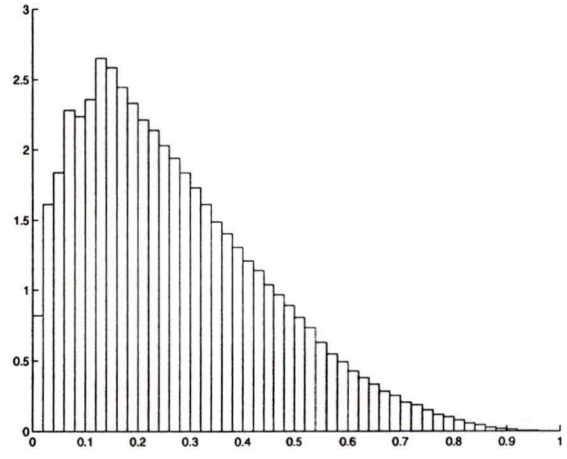

Figure 5.7: Shown here is the Ulam approximate density on a fifty bin partition for the oil drill map with $\gamma = 9.55 \times 10^{-2}$, $\omega = 2.5$. The drill map was defined with 20,000 function evaluations.

energy lost by the drill at the n-th collision is

$$\begin{aligned} E_n &= \frac{1}{2}M\left(c^2 + c^2\left(\frac{dw}{dx}\right)^2\right) + \frac{1}{2}I\Omega_{\text{pre}}^2 - \left(\frac{1}{2}Mc^2 + \frac{1}{2}I\Omega_{\text{post}}^2\right) \\ &= \frac{1}{2}Mc^2\left(\frac{dw}{dx}\right)^2 + \frac{1}{2}I\left(\Omega_{\text{pre}}^2 - \Omega_{\text{post}}^2\right). \end{aligned}$$

where Ω_{post} is the angular velocity after collision, i.e that angular velocity responsible for the fact that the centre of the wheel is moving at constant linear speed c. We assume that the change in kinetic energy due to the rotation is small relative to the change in kinetic energy due to the translation of the wheel. Since this change is dependent on the change of angular velocity of the wheel, the greater the number of teeth the better the approximation

$$E_n \approx \frac{1}{2}Mc^2\left(\frac{dw}{dx}\right)^2.$$

The post collisional velocity is tangential to the base curve, i.e.

$$\vec{v} = \langle c, cf_k'(x_n)\rangle$$

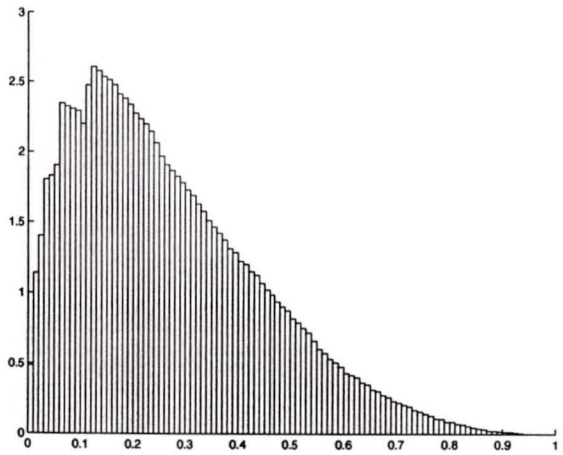

Figure 5.8: Shown here is the Ulam approximate density on a 100-bin partition for the oil drill map with $\gamma = 9.55 \times 10^{-2}$, $\omega = 2.5$. The drill map was defined with 40,000 function evaluations.

and we assume that the energy required for the launch is provided from the drilling mechanism itself, that is input externally.

Suppose for the moment that the entire energy transferred to the rock during the n-th collision is effective in breaking the rock (the extent to which this is not valid is addressed by the efficiency constant $K < 1$ in expression (5.3).

Using the change of variables $x = sT$, $p_k(s) = \frac{f_k(sT)}{R}$ and the formula $c^2 = gR\omega^2$ we obtain

$$f_0(x_{n-1}) = f_0(s_{n-1}T) = Rp_0(s_{n-1})$$

and

$$\frac{df_0}{dx}(x_0) = \frac{1}{T}\frac{df_0}{ds}(s_0T) = \frac{R}{T}\frac{dp_0}{ds}(s_{n-1}).$$

Recall that $p_k(s) = \sqrt{1-\gamma(2s-2k-1)^2} - \sqrt{1-\gamma}$ is the nondimensionalized base curve and therefore

$$w(x, x_{n-1}) = q(s, s_{n-1}) = Rp_0(s_{n-1}) + R(s-s_{n-1})p_0'(s_{n-1}) - \frac{T^2}{2R\omega^2}(s-s_{n-1})^2.$$

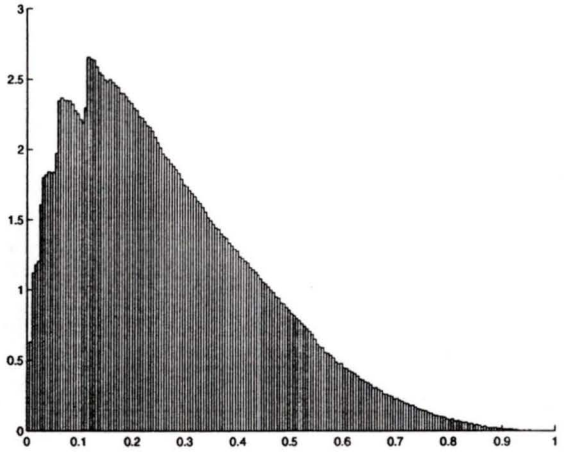

Figure 5.9: Shown here is the Ulam approximate density on a 200 bin partition for the oil drill map with $\gamma = 9.55 \times 10^{-2}$, $\omega = 2.5$. The drill map was defined with 80,000 function evaluations.

Hence

$$\frac{dw}{dx} = \frac{dq}{ds}\frac{ds}{dx} = \frac{1}{T}\frac{dq}{ds}$$

and

$$\frac{dq}{ds}(s_n) = Rp'(s_{n-1}) - \frac{T^2}{R\omega^2}(s_n - s_{n-1}) = Rp'(s_{n-1}) - \frac{T^2}{2R\omega^2}Y(s_{n-1}).$$

This implies that the energy at the n-th landing point is given by

$$E_n \approx \frac{Mc^2R^2}{2T^2}\left(\frac{dp}{ds}(s_{n-1}) - \frac{4\gamma}{\omega^2}Y(s_{n-1})\right)^2$$

where $\gamma = \frac{T^2}{4R^2}$, as defined in Section 3.2.

Thus, using expression 5.2, the average energy per hit is given by

$$\bar{E} \approx \frac{Mc^2R^2}{2T^2}\int_0^1 \left(\frac{dp(s)}{ds} - \frac{4\gamma}{\omega^2}Y(s)\right)^2 g_c(s)\,ds \tag{5.5}$$

where $\omega^2 = \frac{c^2}{gR}$. Using 5.4 and 5.5 we can obtain an estimate for the ratio (5.3). This was done using the Simpson's Rule of numerical integration and the results are shown in the table below.

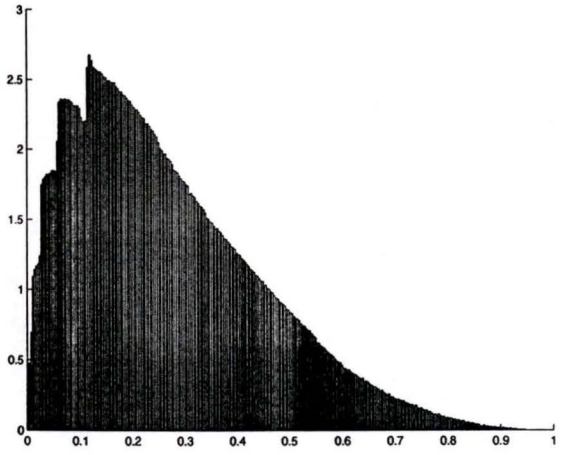

Figure 5.10: The Ulam approximate density on a 300 bin partition for the oil drill map with $\gamma = 9.55 \times 10^{-2}$, $\omega = 2.5$. The drill map was defined with 120,000 function evaluations.

Speed c (m/s)	$\Delta\bar{x}(m)$	$\bar{E}(J)$	$h/K(J/rev)$
0.92	0.0346	0.0243	0.2053
0.93	0.0357	0.0253	0.2071
0.94	0.0356	0.0249	0.2042
0.95	0.0357	0.0250	0.2043
0.96	0.0362	0.0273	0.2207
0.97	0.0369	0.0281	0.2229
0.98	0.0381	0.0294	0.2256
0.99	0.0388	0.0290	0.2188
1.00	0.0400	0.0295	0.2158
1.02	0.0417	0.0297	0.2083
1.05	0.0434	0.0296	0.1990
1.10	0.0458	0.0305	0.1949
1.15	0.0501	0.0330	0.1926
1.20	0.0534	0.0338	0.1852
1.40	0.0698	0.0420	0.1757
1.60	0.0883	0.0513	0.1696
3.00	0.2832	0.1510	0.1563
5.00	0.7642	0.4018	0.1536

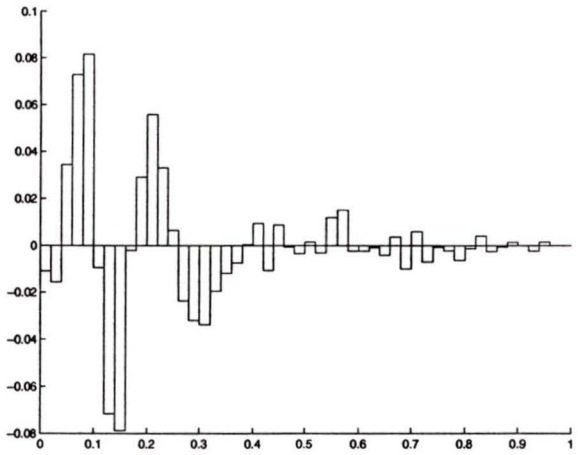

Figure 5.11: The difference-error function between the 300-bin and 50-bin estimates computed over 120,000 and 20,000 function evaluations respectively, when $\omega = 2.5$.

In Table 5.3 it can be observed that as the speed c increases, the average energy per hit shows a general increase. However this increase is at the expense of the number of hits per revolution, i.e. the average energy per revolution drops, because of the excessive number of revolutions between hits. We remark that the peak area has been fairly carefully computed.

Figure 5.13 shows the graph h/K vs. rotations per minute, *rpm*. The expression for $\rho = rpm$ in terms of speed c is

$$\rho = 60c\left(\frac{1}{2\pi R}\right)\left(\frac{2R}{d}\right) \approx 205.4c,$$

where the factor $\left(\frac{1}{2\pi R}\right)$ converts the speed c from units *meters/sec* to *wheel rotations/sec*, and $\left(\frac{2R}{d}\right)$ converts from *wheel rotations* to *drill bit rotations.*

Our result supports Lasota and Rusek's results and those observed in the field. Namely, as the speed increases the efficiency of the drill has the asymptotic behaviour $h/K \to 0.15$ Jrev^{-1}. Furthermore, the graph shows that the peak efficiency occurs when $c = 0.98$ ms^{-1}. Then $h/K = 0.2256$ Jrev^{-1}. The analogous run on 200 bins and 80,000 points gives a value of $h/K = 0.2235$ Jrev^{-1} when $c = 0.98$ ms^{-1}. Due

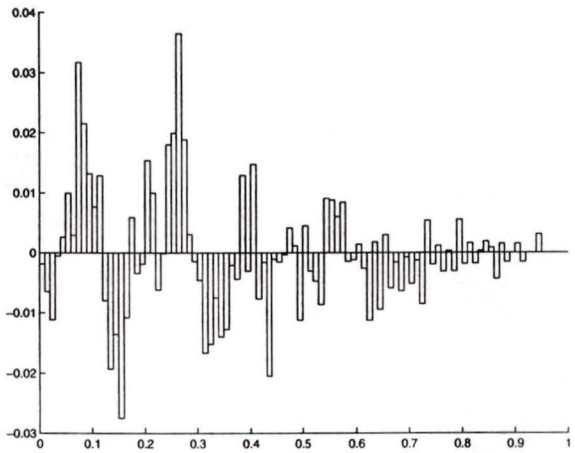

Figure 5.12: Shown here is the difference-error function between the 300-bin and 100-bin estimates computed over 120,000 and 40,000 function evaluations respectively, when $\omega = 2.5$.

to the laborious nature of these evaluations and the negligible error, the data is based on 50 bins, and the drill transformation is defined on 20,000 points. Observe that the asymptotic value of h/K is 66% of the peak value of $h/K = 0.2256$ Jrev^{-1}.

5.4 Conclusion

In this chapter we estimated the invariant density function using Ulam's method, known for its fast convergence. The reliability of this method was observed through several numerical estimates for different speeds. Some discontinuities of the invariant density function were observed and discussed. Thus, unlike the assumption by Lasota and Rusek of the continuous γ-distribution, in this work we used the raw estimate from Ulam's method for further analysis. Once the estimate was computed, the mean energy per revolution was determined as a function of the Froude number ω^2, using the Birkhoff ergodic Theorem. The graph of mean energy per revolution vs. rotations per minute was plotted for different values of the speed c, and we

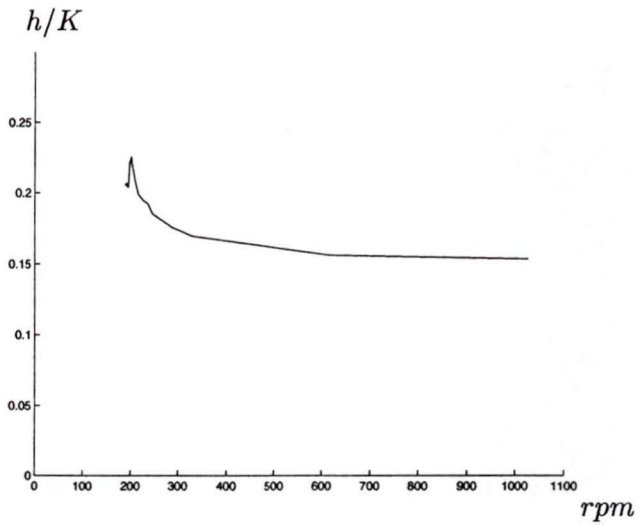

Figure 5.13: Shown here is the graph of h/K vs. rpm.

observed the asymptotic behaviour of the dynamics of the drill. Namely, as the speed increases, the amount of energy lost by the drill approaches the limiting value of 0.15 Jrev^{-1}. Furthermore, the maximum amount of energy transferred from the drill was found to be 0.2256 Jrev^{-1}, occurring when the speed is $c = 0.98$ ms^{-1}. This means, that the limiting value is 66% of this maximum amount of energy. In Lasota-Ruseks' results, this percentage was found to be 60%. The discrepancy is perhaps due to the assumption of the gamma distribution in that work.

Chapter 6

Summary Of Results And Future Work

6.1 Summary

The invariant density function plays a central role in predicting the wear-and-tear of the drill and the uniformity and rate of the drilling. In this thesis we have presented two ways of computing an estimate for this function.

In Chapter 2 we discussed the Birkhoff Ergodic method for computing the invariant density function. Applied to the drill map derived in Chapter 3, this produced the estimates in Figures 3.11, 3.12 and 3.13. We observed that this method is sensitive to slight perturbations in the choice of initial point of launching, and very labour intensive for long orbits. Due to the numerous function evaluations along the orbit of the initial point, computer round off error is compounded, making estimates based on longer orbits less reliable. This established the need for Ulam's method, which was presented in Chapter 4. Applied to the drill map this method showed better stability in the estimates and gave confidence for the overall shape of the frequency of hits. The energy formula (5.5) allowed us to predict the efficiency of the drill for various linear speeds. The speed which yields highest drilling efficiency was computed, and the asymptotic efficiency (as a function of speed) was calculated.

Although counter-intuitive, we attempt to make sense of this behaviour. Consider for a moment that launching occurs from a flat surface (as opposed to the base curve). Then using a simple projectile motion argument it can be shown that the distance between points of contact varies as the square of the speed. Of course, the kinetic energy also varies as the square of the speed, thus we expect that in this case the ratio between energy and distance would be constant. Now, returning to the model of the drill, similar behaviour can be expected for high speeds, since the base curve is of relatively small curvature. In other words, the higher the linear speed of the wheel, the less noticeable the curvature of the base curve. In contrast, when the speed is lower, the projectile described by the wheel is more sensitive to the curvature of the base curve, explaining the peak in Figure 5.13. This behaviour has been observed over the years of drilling practical experience. It was first studied by Lasota and Rusek [8], who provided a mathematical explanation to this phenomenon. In this thesis, we presented more numerically accurate evidence in support of Lasota and Rusek's work.

6.2 Future Work

The stability of Ulam's method is apparent, still with every estimate one asks how close we are to the true invariant density function. In his dissertation, [10], Rua Murray answered this question for a class of maps with certain characteristics. For these maps he was able to give an explicit upper bound on the approximation error in Ulam's method. He found that the n^{th} Ulam approximate density (i.e. one based on n bins) is within $C\frac{\log n}{n}$ of the true invariant density, measured in L^1 norm, where C is a constant which has an explicit formula depending only on the map itself. Unfortunately, the drill map does not fit into this class of maps, thus the study of the error bounds of the Ulam approximate density remains open.

In Chapter 4 we discussed Ulam's method and Li's theorem about convergence of Ulam's method. We noted that in fact the drill map cannot been analytically proven to satisfy all of the hypotheses of Li's theorem. An alternative way of obtaining the invariant density function would be to apply Ulam's method on the induced map, which does satisfy the conditions in question. A comparative analysis on the relative efficiency of the two methods would make an interesting future project.

Appendix A

Pseudocode

A.1 Range Map

The Range map L discussed in Chapter 3 is determined by calling the routine *Getmap*, which in turn calls the subroutine *Drillmap*, both described in this section.

Consider a drill bit of mass M, with a wheel of radius R, distance between teeth T and number of teeth N. Suppose g is the acceleration due to gravity, and c is the linear velocity of the wheel. This set of parameters will be referred to as the drill parameters.

A.1.1 Getmap Routine

This routine will be called in both the Birkhoff method and Ulam's method routine, in each case before computing the invariant density function.

Given the drill parameters and a launch point $x \in [0,1]$ this routine determines the range map $L(x) : [0,1] \to (0,\infty]$.

GLOBAL VARIABLES: Drill parameters, $\gamma = \frac{T^2}{4R^2}$, $\omega^2 = \frac{c^2}{gR}$

INPUT: Launching point x

- Step 1: Determine the maximum launching distance K, thus restricting the range of the map $L : [0,1] \to [0,K]$. This is the point of contact of the base

curve with the projectile curve described when launched at $x = 0$. A simple substitution leads to

$$K \approx \frac{\omega^2}{\sqrt{1-\gamma}}.$$

The value of K also gives the number of branches that the map L will have. Namely, number of branches $= B \stackrel{\text{def}}{=} \lceil K \rceil - 1$, where $\lceil K \rceil$ is the smallest integer i, such that $i \geq K$.

- Step 2: While $n < B$, call subroutine *Drillmap* with input parameters launching point x and branch number n.

  CASE 1: If landing point does not occur on the current hump, $[n, n+1]$, *Drillmap* returns a default value of $n+2$ (i.e. outside the admissible range for the landing points on this hump). This default value tells the routine to move to the next hump (increment n to $n+1$) and check again. If beyond the last branch number, inform the user of an error.

  CASE 2: If landing does occur on the current hump, then *Drillmap* returns the approximate value of landing point, $L(x)$. Thus in this case we do not need to iterate to the next hump; the routine stops.

A.1.2 Drillmap Routine

This routine is concerned with finding the approximate value of the landing point $L \in [n, n+1]$, given launching point $x \in [0, 1]$, and branch n to search in. The routine checks if this occurs on the given hump $[n, n+1]$ and gives the approximate root of the function

$$y = \text{(projectile curve described when launched at } x\text{)} - \text{(base curve)}.$$

If the given hump $[n, n+1]$ is not the right place to search this root, the routine returns a value outside the admissible region, so that the driver routine knows to

move to the next branch.

GLOBAL VARIABLES: Drill parameters, $\gamma = \frac{T^2}{4R^2}$, $\omega^2 = \frac{c^2}{gR}$

INPUT: Launching point x, and branch number n.

- Step 1: Set up the function that needs to be minimized, $y(x, L, n)$,

$$y = \sqrt{1-\gamma(2x-1)^2} - \frac{2\gamma(L-x)(2x-1)}{\sqrt{1-\gamma(2x-1)^2}} - \frac{2\gamma(L-x)^2}{\omega^2} - \sqrt{1-\gamma(2L-2n-1)^2}.$$

Steps 2 and 3 are a root finding routine which approximates the value of L where $y = 0$ for fixed x and n. Step 2 determines if the root exists. In case it does, Step 3 finds its approximation. There are three possibilities for this root.

1). There are two real roots, $r_1 < r_2$. In this case the routine finds $L = r_1$, where $r_1 \in [n, n+1]$.

2). There is one real root, r. This is the case when one branch ends and another begins. That is, the projectile curve hits the base curve tangentially at the single root, and for any $\Delta x > 0$, the projectile curve described for launching point $x + \Delta x$ intersects the base curve in hump $[n+1, n+2]$. In this case the routine described in Steps 2 and 3 returns an approximation to the single root $r \in [n, n+1]$.

3). There are no real roots. The routine returns a value outside the admissible region, indicating to the driver routine that the wrong branch was searched, which in turn will iterate on the branch number and search again.

REMARK: The *Drillmap* routine is called iteratively. That is, the value of the function y on the given hump will always be positive, unless the root in question belongs to this interval. In other words, this routine does not get called when the value of the branch n is greater than the value of the root (in which case $y(s) < 0$ for all $s \in [n, n+1]$).

- Step 2: In this step we determine if the given hump contains the root in question, by minimizing the function y on this interval and checking if this minimum value is negative. It returns a value for the position s where that negative y value occurs. If this subroutine finds only positive values for y (minimum is positive), it returns the value of $s = n + 2$, indicating to the driver routine that there are no real roots for this value of n.

  Initialize the outside range $[x_0, x_3] = [n, n+1]$ and the inside range $[x_1, x_2] = [(n + 1/2) - (1 - \rho)(x_2 - x_0), n + 1/2]$, where $\rho = (\sqrt{5} - 1)/2$. Here the golden ratio is used in the bisection method (see [11]), for proven efficiency of minimization. Evaluate the function y at the end points of the inside range, i.e at x_1 and x_2.

  While no negative value for y has been detected repeat:

  Case 1. If the value of $y(x, x_1, n) > y(x, x_2, n)$, move the outside interval to $[x_0, x_3] = [x_1, x_3]$, and the inside interval to $[x_1, x_2] = [x_2, (\rho)x_0 + (1 - \rho)x_3]$. Compare the values of y at the end points of the iterated inside interval.

  Case 2. If $y(x, x_1, n) < y(x, x_2, n)$, move the outside interval $[x_0, x_3] = [x_0, x_2]$, and the inside interval $[x_1, x_2] = [(\rho)x_1 + (1 - \rho)x_0, x_1]$.

  Break when a negative value for y has been detected, or the distance between the outside interval has become smaller than or equal to $10^{-5}(|x_1| + |x_2|)$. In the former case return the value $xstar \in [n, n+1]$ where the negative value of y occurs, and in the latter case return $xstar = n + 2$, indicating to the driver routine that it needs to move to the next branch.

  If the value returned in Step 2 is negative, then we know that there is at least one root. In this case we will find an approximation for the root in $[n, xstar]$, since we want the smaller of possibly two roots. In this case Step 3 performs

a root finding routine to approximate its value.

- Step 3: Perform the secant method to find the root in $[n, xstar]$, with an accuracy of $xacc = 10^{-5}$. We are guaranteed of the existence of this root by Step 2.

  (1) Initialize $x_1 = n$ and $x_2 = xstar$.

  (2) Evaluate $f_1 = y(x, x_1, n)$ and $f = y(x, x_2, n)$.

  (3) Now we compare their absolute values. If $|f_1| < |f|$, return with $x_{\text{temp}} = x_1$, otherwise $x_{\text{temp}} = x_2$.

  (4) Preset f to be the smaller and f_1 to be the larger of the two values. Let

  $$dx = (x_1 - x_{\text{temp}})\frac{f}{f - f_1}.$$

  Then let $f_1 = f$ and $f = y(x, x_{\text{temp}} + dx, n)$. Repeat (4) in an iterative manner until $|dx| < xacc$ or $f = 0$.

  (5) Return the final value of $x_{\text{temp}} \approx L$.

A.2 Birkhoff Method Routine

The *Birkhoff* routine described in this section produces the invariant density function of the Range map using the Birkhoff method discussed in Chapter 2. The method is characterized by the point of initial launch, the length of its orbit, and the number of bins over which the invariant density will be approximated.

GLOBAL VARIABLES: Drill parameters

LOCAL VARIABLES:

1) Number of bins = *numbins*,

2) Initial point of launching = *xposition*,

3) Length of orbit to be computed starting at $xposition = numiters$

- Step 1: Initialize all of the bins to start their count at 0. Thus at this point, Bin $\#1 = [0, 1/numbins]$ has a total of 0 hits, as well as Bin $\#i = ((i-1)/numbins, i/numbins]$ for $i = 2 \ldots (numbins+1)$. Note that only Bin #1 is closed.

- Step 2: Iterate on $i = 1$ to $numiters$. Beginning with $xposition$, determine the point of landing, $yposition$, by calling the *Getmap* routine. Change the returned value to $yposition \,(mod\, 1)$. This value of $yposition$ belongs to Bin with index $\#\left(\lceil yposition \times numbins \rceil\right)$. Thus, increase the count inside this bin by 1. Reassign $xposition = yposition$ and repeat Step 2 until every hit of the orbit of length $numiters$ has been assigned to its appropriate bin.

- Step 3: The resulting histogram needs to be renormalized to have Lebesgue measure one. If C is the renormalization constant, then

$$\frac{1}{numbins} \sum_{i=1}^{numiters} C\,(\text{count in bin } (i)) = C\left(\frac{numiters}{numbins}\right) = 1.$$

  Therefore the normalization constant is $C = numbins/numiters$.

- Step 4: For $i = 1$ to $numbins$, output each of the $numbins$ components of the distribution vector, where component $i = (\text{count in bin } i)(numbins/numiters)$.

- Step 5: Plot the histogram with components determined in Step 3 to obtain a picture of the distribution vector.

A.3 Ulam's Method Routine

In this section we describe the numerics behind the *Ulam* routine, which produces an estimate for the invariant density vector using Ulam's method, described in Chapter

4. In this method, the variables are the number of points that define the drill map, and the number of bins over which the approximation will be produced. Recall that here the matrix of transition probabilities corresponding to the the drill map must be set up. The eigenvector belonging to the dominant eigenvalue, $\lambda = 1$, is the approximation of the invariant density vector.

GLOBAL VARIABLES: Drill parameters

LOCAL VARIABLES:

1) Number of bins = *numbins*,

2) Number of points that describe the drill map = *numiters*

- Step 1: Initialize the count in each of the *numbins* (the components of the invariant density vector) to 0.

- Step 2: Initialize all of the matrix entries to $q(i,j) = 0$, for $1 \leq i, j \leq numbins$.

- Step 3: For $i = 1$ to $(numiters + 1)$, compute the value of the landing point using the *Getmap* routine for each of the *numiters* points x_i spaced equally in the unit interval. Determine the corresponding point y_i after computing the returned value *mod* 1. Increase the count $q(xbin, ybin)$ by 1, where $xbin = \lceil x_i \times numbins \rceil$ and $ybin = \lceil y_i \times numbins \rceil$. This counts the number of points that after one iteration of the drill map move from Bin_{xbin} of the domain into Bin_{ybin} of the range. That is, this determines the measure of the set $\text{Bin}_{xbin} \cap S^{-1}(\text{Bin}_{ybin})$.

- Step 4: Make sure that all of the points are accounted for. Initialize $countpoints = 0$. For $i = 1$ to *numbins* and , $j = 1$ to *numbins*, $countpoints = countpoints + q(i,j)$. If at the end of this counting subroutine $countpoints \neq numiters + 1$, print out a warning message, that not all of the points have been accounted for.

- Step 5: Form the row stochastic matrix $\{p(i,j)\}$ defined by

$$\{p(i,j)\} = \left\{ \frac{q(i,j)}{\sum_{i=1}^{numiters+1} q(i,j)} \right\}.$$

- Step 6: In this step we compute the eigenvector of the dominant eigenvalue $\lambda = 1$ of the transition matrix. This is done in two ways, so that any discrepancies can be detected. Both methods are relatively fast.

  Method 1. Get Matlab to compute all of the eigenvalues and eigenvectors and extract the eigenvector that corresponds to the dominant eigenvalue $\lambda = 1$. Suppose the eigenvector appears in the column with index *evector*.

  Method 2. Presumably the matrix of transition probabilities is not only row stochastic, but also irreducible. Thus, by Theorem 4.6, high powers of the matrix converge to one with columns the eigenvector of interest.

- Step 7: Form the histogram, after renormalization. If C is the renormalization constant, then

$$\begin{aligned} \sum_{i=1}^{numbins} & C \text{ (sum of entries in row } (i), \text{ column } evector) \frac{1}{numbins} \\ = \quad & C \, \frac{||evector||}{numbins} = 1, \end{aligned}$$

  which implies $C = numbins/||evector||$, where $||evector||$ is the L^1 norm of the dominant eigenvector.

  Thus, for the invariant density vector we have for $i = 1$ to $numbins$, component $(i) = C$ (entry in row (i), column *evector*). Output these values and plot the histogram.

Bibliography

[1] Seneta, E. (1973). *Non-negative matrices.* New York: Academic Press Inc.

[2] H. L. Royden, (1988). *Real Analysis, Third Edition.* New Jersey: Prentice-Hall, Inc.

[3] Feller, William (1957). *An Introduction to Probability Theory and Its Applications.* New York: John Wiley & Sons, Inc.

[4] Li, T-Y (1974). *Finite Approximation to The Frobenius Perron Operator. A Solution To Ulam's Conjecture.* Journal Of Approximation Theory 17:177-186

[5] Ulam, S. (1960). *A Collection of Mathematical Problems* Interscience Publishers

[6] Billingsley, P. (1968). *Convergence Of Probability Measures* New York: John Wiley

[7] Lasota, A. & Yorke, J. A. (1973). *On the Existence of Invariant Measures for Piecewise Monotonic Transformations.* Transactions of the American Mathematical Society, 186 (December).

[8] Lasota, A. & Rusek, P. (1974). *Application Of Ergodic Theory to the Determining of Cogged Bit Efficiency.* Warsaw, Archiwum Górniktva, Tom XIX, No.3.

[9] Boyarsky, A. & Góra, P. (1997). *Laws Of Chaos: Invariant Measures and Dynamical Systems in One Dimensional* Boston: Birkhäuser

[10] Murray, R. (1991). *Discrete Approximation of Invariant Densities.* disertation for the degree of Doctor of Philosophy, University of Cambridge, August 1997

[11] Burden, R. & Faires, J. (1985). *Numerical Analysis* Boston, Mass: Prindle, Weber & Schmidt

[12] Singe, J. & Griffith, B. (1959). *Principles of Mechanics.* McGraw-Hill Book Company, Inc.

Vita

Surname:	Davidova
Given Names:	Adriana
Place of Birth:	Sofia, Bulgaria
Date of Birth:	February 4th, 1974

Educational Institutions Attended

University of Victoria, Victoria	1994-2001

Degrees Awarded

B. Sc. (Mathematics) University of Victoria	1998

Honours and Awards

Departmental Fellowship	Sep 1998 - Aug 1999
Departmental Fellowship	Sep 1999 - Aug 2000
Departmental Fellowship	Sep 2000 - Dec 2000

PUBLICATIONS

Contaminant Transport in Municipal Water Systems, PIMS Industrial Problem Solving Workshop, January 2000

Partial Copyright License

I hereby grant the right to lend my thesis to users of the University of Victoria Library, and to make single copies only for such users, or in response to a request from the Library of any other university or similar institution, on its behalf or for one of its users. I further agree that permission for extensive copying of this thesis for scholarly purposes may be granted by me or a member of the university designated by me. It is understood that copying or publication of this thesis for financial gain shall not be allowed without my written permission.

TITLE OF THESIS:

THE DYNAMICS OF A ROCK DRILL

Author: [redacted]

ADRIANA DAVIDOVA

20/10/01

(20/10/01)